A new insight on direct actions of Granulocyte-Colony Stimulating Factor in the myocardium

Inaugural-Dissertation

to obtain the academic degree

Doctor rerum naturalium (Dr. rer. nat.)

Department of Biology, Chemistry and Pharmacy

of **Freie Universität Berlin**

by

Ana Catarina Ribeiro Carrão

Portugal

28th January, 2009

Reviewers:

1st Reviewer: Prof. Petra Knaus

2nd Reviewer: PD Dr. Ivo Buschmann

Date of defence: 4th June 2009

Acknowledgments:

I would like to thank Prof. William Chilian for his unquestionable support and for being an earnest mentor. I would also like to thank my family who even from so far away was always there for me with a word of comfort and wisdom. To Dr. Clemens Gruber my most dear appreciations for his critical reading and especially his companionship; without his support I would not have made it so far.

Directory

Page

List of figures

List of tables

Summary

Granulocyte colony-stimulating factor (G-CSF) is a known hematopoietic cytokine that promotes proliferation and differentiation of neutrophil progenitors. Since G-CSF is recognized to ameliorate myocardial ischemic injury, it was projected that this effect would translate into stimulating myocardial adaptations similar to the ones promoted by ischemic preconditioning. Accordingly, it was hypothesized that G-CSF stimulates coronary collateral growth (CCG) in a rat model of repetitive episodic ischemia (RI). Groups of animals were subjected to repetitive episodes of 40 sec left anterior descending coronary artery (LAD) occlusion every 20 min for 2h20min, 3 times/day for a total period of 5 days. CCG was deduced from collateral-dependent flow, i.e., flow to LAD dependent-region determined with neutron activated microspheres during occlusion, and expressed as the increase in the ratio between collateral-dependent and normal zone flows from the initial measurement to that of after 5 days of RI. Following RI, G-CSF treatments (100 μg/Kg/day, s.c.) increased CCG (0.47 ± 0.15 *versus* vehicle 0.14 ± 0.06, $P<0.01$). Surprisingly, G-CSF treatment without RI increased CCG (0.57 ± 0.18, $P<0.01$ *vs.* vehicle) equal to G-CSF + RI. Because redox signalling is known to be critical for CCG and neutrophils are a rich source of NADPH oxidase and reactive oxygen species (ROS), it was further hypothesized that G-CSF stimulates production of ROS. ROS were evaluated by dihydroethidine (DHE) fluorescence, which was injected in the left ventricle (60 μg/kg) during two consecutive episodes of ischemia. DHE fluorescence was double in G-CSF + RI *vs.* vehicle + RI ($P<0.01$), and even higher values were found in G-CSF without RI stimulus ($P<0.01$). Interestingly, immunostaining with a specific neutrophil marker, myeloperoxidase, showed that the DHE signal did not localize in neutrophils but it appeared in cardiac myocytes. To unequivocally determine if G-CSF stimulated ROS production in cardiac myocytes, isolated cardiac myocytes were studied and it was found that the cytokine stimulates the production of ROS and angiogenic factors that are able to promote tube formation in human coronary artery endothelial cells (HCAECs). In addition to affecting neutrophils, G-CSF directly targets cardiac myocytes to produce ROS and angiogenic factors. This direct action of G-CSF in cardiomyocytes shows how this cytokine plays a pivotal role in triggering adaptations of the heart to ischemia including growth of the coronary collaterals.

Zusammenfassung

Granulozyten-Kolonie-stimulierender Faktor (engl. granulocyte colony-stimulating factor, G-CSF) ist ein bekanntes hämatopoetisches Zytokin, das die Proliferation und Differenzierung neutrophiler Voläuferzellen fördert. Da G-CSF den Verlauf ischämischer Myokardläsionen positiv beeinflussen kann, wurde angenommen, dass dieser Effekt auf der Stimulation myokardialer Anpassungsvorgänge ähnlich jener nach ischämischer Präkonditionierung beruht. Entsprechend wurde die Hypothese aufgestellt, dass G-CSF in einem Modell repetitiver episodischer Ischämie (RI) in der Ratte koronares Kollateralwachstum (engl. coronary collateral growth, CCG) stimulieren würde. Einzelne Versuchstiergruppen wurden dafür repetitiven Episoden einer 40 Sekunden andauernden Okklusion des Ramus interventricularis anterior der linken Koronorarterie (engl. left anterior descending coronary artery, LAD) ausgesetzt, die für eine Dauer von insgesamt 5 Tagen drei mal pro Tag für 2h 20min alle 20 Minuten wiederholt wurden. CCG wurde dann vom von Kollateralen abhängigen Blutfluss, d.h. vom mit Hilfe von Neutronen-aktivierten-Mikrosphären bestimmten Blutfluss im Strombahngebiet der LAD während der Okklusion, hergeleitet und als Steigerung des Verhältnisses der Durchblutung zwischen LAD- und nichtokkludierten Strombahngebieten von der ursprünglichen Messung zu der Messung 5 Tage nach RI ausgedrückt. Unter RI führte die Gabe von G-CSF (100 μg/kg/d, s.c.) zu gesteigertem CCG (0.47 ± 0.15 *versus* Vehikel 0.14 ± 0.06, $P<0.01$). Überaschenderweise steigerte G-CSF ohne RI das CCG (0.57 ± 0.18, $P<0.01$ *vs.* Vehikel) wie G-CSF + RI. Da neutrophile Granulozyten reichlich NADPH Oxidase und reaktive Sauerstoffspezies (engl. reactive oxygen species, ROS) enthalten und letztere für das Kollateralwachstum essentiell sind, wurde weiter angenommen, dass G-CSF die Bildung von ROS stimuliert. Das Vorhandensein von ROS wurde dafür anhand der Fluoreszenz von Dihydroethidin (DHE) überprüft, welches während zwei konsekutiver ischämischer Episoden in den linken Ventrikel injiziert wurde. DHE-Fluoreszenz war doppelt so stark in G-CSF + RI gegenüber Vehikel + RI ($P<0.01$), und sogar noch höhere Werte wurden für G-CSF ohne RI gemessen ($P<0.01$). Interessanterweise zeigten Immunfärbungen mit Myeloperoxidase als spezifischem Neutrophilen-Marker, dass das DHE Signal nicht in Neutrophilen, dafür aber in Kardiomyozyten lokalisiert war. Um eindeutig festzustellen, ob G-CSF die ROS-Produktion in Kardiomyozyten stimuliert, studierten wir isolierte

Kardiomyozyten und fanden heraus, dass G-CSF die Produktion von ROS und angiogenetischen Faktoren stimuliert, welche ihrerseits die Formation tubulärer Strukturen durch koronare Endothelzellen (engl. human coronary artery endothelial cells, HCAECs) fördern. Neben seinem Effekt auf neutrophile Granulozyten fördert G-CSF also auch direkt die Produktion von ROS und angiogenetischen Faktoren in Kardiomyozyten. Dieser direkte Einfluss von G-CSF auf Kardiomyozyten unterstreicht die entscheidende Rolle dieses Zytokins in der Auslösung adaptiver Mechanismen des Herzmuskels unter Ischämie, einschließlich des Wachstums koronarer Kollateralen.

1. Introduction

Chapter I: G-CSF and its biological actions

Granulocyte-colony stimulating factor (G-CSF) is a polypeptide growth factor that regulates the production of neutrophilic granulocytes. This physiological process serves as the foundation for critical host defence systems and occurs on a large scale *in vivo*. An adult of average size will produce approximately 120 billion granulocytes per day simply to replace normal losses[1]. This enormous production capacity may be increased by at least 10-fold under stress conditions such as infection. G-CSF plays a pivotal role in the basal regulation of neutrophil production as well as functioning as a primary regulatory factor controlling the neutrophil response to inflammatory stimuli. Also, G-CSF exhibits other biological activities and G-CSF-induced hematopoietic stem cell mobilization is widely used clinically for peripheral blood stem cell transplantation. In animal models G-CSF has been shown to prevent left ventricular remodelling and dysfunction after acute myocardial infarction. Although it is controversial whether bone marrow stem cells mobilized by G-CSF can differentiate into cardiac myocytes, G-CSF-induced angiogenesis is indeed recognized in the infarcted heart. Therefore, G-CSF may be used as a novel protective and regenerative agent on injured myocardium. Although the effects of G-CSF on the progression of atherosclerosis are still unclear, there is a possibility that G-CSF will become a promising therapy for ischemic heart disease. G-CSF possesses unique and interesting characteristics among the family of hematopoietic growth factors. This chapter will summarize the current state of knowledge of the structure and function of G-CSF and its receptor.

I.1 Identification of G-CSF and its gene

The identification of CSFs was made possible by cell culture assays for hematopoietic progenitor cells developed in the mid 1960s by Metcalf and his colleagues[2]. These *in vitro* systems showed that the survival, proliferation, and differentiation of immature hematopoietic cells were dependent on the continued presence of humoral factors, which was collectively termed "colony-stimulating activity" (CSA)[3]. Before the purification of individual factors, early sources of CSA

included media that was conditioned by stimulated cultures of normal blood or certain tumour cells. It was initially unclear whether these complex mixtures contained both individual factors specific for proliferation and/or separate factors that would specifically induce differentiation. Further investigation showed that many of these biological activities were attributable to the simultaneous presence of multiple factors in the crude medium. In 1978, Byrne *et al.*[4] reported that medium that was conditioned by mouse heart tissue was found to contain CSFs which produce *in vitro* colonies of granulocytes and/or macrophages. Purification of these CSFs proved difficult and for many factors, expression, cloning and production of recombinant proteins were required to completely define the unique biological properties of individual CSFs. G-CSF was probably first identified as having a distinct activity by Burgess and Metcalf[5], not by its ability to stimulate proliferation, but rather by the capacity of postendotoxin-treated mouse serum to induce differentiation in a murine leukemic cell line. Therefore, Metcalf initially termed G-CSF a granulocyte-macrophage differentiation factor (GM-DF) and he noted it to be related to (or being the same as) the so-called macrophage- and granulocyte-inducing proteins, reported by Lotem *et al.*[6]. GM-DF was shown to be separate from GM-CSF, which had been partially purified in the late 1970s. This distinction was experimentally determined by the generation of neutralizing antiserum that could block the effects of GM-CSF, but which failed to block the activity of GM-DF. GM-DF was then shown to co-purify with a novel medium that selectively stimulated the formation of granulocytic colonies from normal hematopoietic progenitor cells *in vitro*[7] and, after further purification, this factor was ultimately renamed G-CSF[8]. Nicola *et al.*[8] described the biochemical characteristics of murine G-CSF in 1983, as a hydrophobic glycoprotein with an apparent molecular weight of 24-25 Kd, containing a neuraminic acid moiety and at least one internal disulfide bond that was necessary for its biological activity. After the identification of the murine G-CSF, a human molecule with analogous activities was discovered[9]. Both the proliferation- and differentiation-inducing activities of the murine and human G-CSF molecules cross species boundaries, in contrast to other hematopoietic growth factors such as GM-CSF or interleukin-3 (IL-3) which are active in a species-specific manner on the neutrophilic cell lineage[3]. In 1986, Nomura *et al.*[10] finally described G-CSF as a molecule that specifically induces growth of the neutrophilic granulocyte lineage of cells.

Further understanding of the biological and biochemical properties of G-CSF was greatly facilitated by cloning of the gene encoding G-CSF and the production of

recombinant protein for study[11, 12]. Southern blot analysis of genomic human DNA showed that G-CSF is encoded by a single gene[11, 13], and further studies determined that this single gene is located on chromosome 17q11-22[14, 15]. The genomic structure of the human G-CSF gene was determined by Nagata *et al*[13], revealing that G-CSF gene consists of 5 exons spread over a locus of approximately 2.3 kb (**Fig. 1**). At the 5'-terminus of the second intron, two donor splice sequences are present in the tandem, only 9 bp apart. The localization of human G-CSF on chromosome 17 differs from that of several other human hematopoietic growth factors such as GM-CSF, IL-3, IL-4 and IL-5, which are clustered on the long arm of the chromosome 5[16]. Following the description of the cDNA for human G-CSF, the murine G-CSF was cloned by cross-hybridization with a human G-CSF cDNA probe. The murine G-CSF gene is highly homologous with the human gene, with 69% nucleic acid sequence homology in both coding and non-coding regions, and a 73% sequence homology in the predicted amino acid sequence of the protein[17]. The rat sequence of the G-CSF gene shares a high degree of identity in coding and non-coding regions with both the murine (85%) and human G-CSF (74%)[18].

The human G-CSF gene is distantly related to the IL-6 gene. The number, location and size of the introns and exons that comprise these two genes are similar. Additionally, the amino acid sequences of G-CSF and IL-6 share some localized homology. Between amino acid residues 20 to 85 of G-CSF, the positions of 17 residues match with residues located between positions 28 to 91 of the IL-6 molecule, which yields a sequence homology for this region of 26%[3]. Additionally, the positions of four cysteine residues are precisely conserved between G-CSF and IL-6 in this region of relative homology. The tertiary structure of G-CSF may be quite similar to that of IL-6, particularly if intra-chain disulfide bridges are similarly located within these molecules. Thus, it is possible that the genes encoding G-CSF and IL-6 may have arisen from a gene duplication event after which they have subsequently diverged. There is no linkage of chromosomal localization between G-CSF and IL-6, because human IL-6 is located at chromosome 7p15[19].

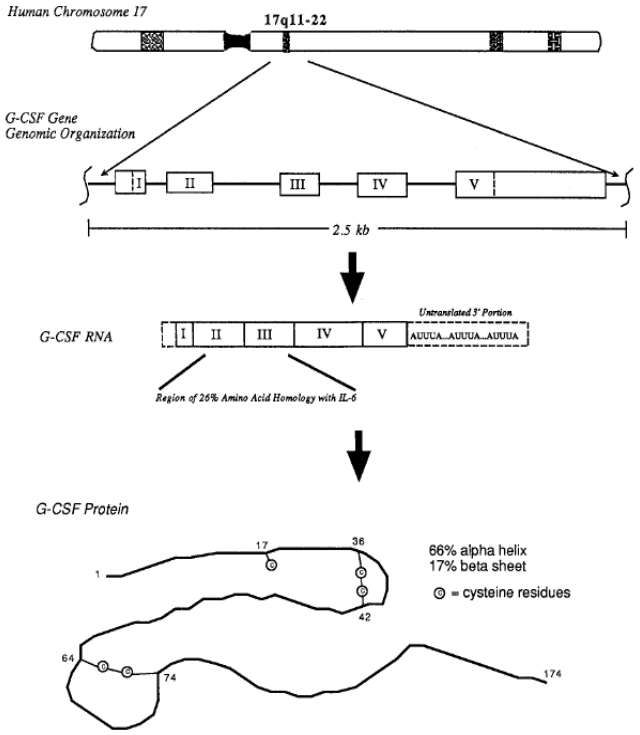

Fig. 1 – Molecular organization of the gene encoding human G-CSF, structure of the G-CSF RNA transcript, and secondary structure of the native human G-CSF protein.[8]

I.2 Production of G-CSF: cellular sources and physiological roles

In 1994, Lieschke *et al.*[20] were the first group to create a G-CSF knock-out mouse (genotype $GCSF^{-/-}$). These mice were viable, fertile and superficially healthy, but had chronic neutropenia, i.e., peripheral blood neutrophil levels were 20 to 30% of the level found on the wild-type mice. In the bone-marrow of $GCSF^{-/-}$ mice, they found that granulopoietic precursor cells were reduced by 50% and there were also reduced levels of granulocyte, macrophage and blast progenitor cells. Despite G-CSF deficiency, mature neutrophils were still present in the blood and bone-marrow, indicating that other factors could support neutrophil production *in vivo*. An important finding in this study relates to the markedly impaired ability of this $GCSF^{-/-}$ mice to control bacterial infection, indicating that G-CSF is indispensible for not only maintaining the normal quantitative balance of neutrophil production but also has a role in "emergency" granulopoiesis *in vivo*.

G-CSF production is increased sharply in response to bacterial infection and cell-mediated immune responses[3]. Bacterial products, such as endotoxin, or secondary mediators induced during infections [tumour necrosis factor-α (TNF-α), IL-1, and interferon-γ (IFN-γ)], are major stimulators of G-CSF production *in vivo* and result in a rapid but transient elevation of G-CSF serum levels[21-23]. As a member of the CSF family of hormone-like glycoproteins, G-CSF has the ability to regulate hematopoietic cell proliferation and differentiation specifically by influencing the proliferation, survival, maturation and functional activation of cells from the neutrophilic granulocyte lineage[24, 25]. The immature neutrophils that arise from bone marrow follow a process that involves proliferation, differentiation along the granulocyte lineage and terminal maturation into functional neutrophils. Many other hematopoietic growth factors like stem cell factor (SCF), IL-3, GM-CSF, IL-6, have been shown to be positive regulators of granulopoiesis and act at different stages of myeloid cell development. But, G-CSF is unique among the regulators of granulopoiesis, because it not only stimulates the proliferation but also potently induces the terminal maturation of myeloid progenitor cells to neutrophilic granulocytes[1].

G-CSF is produced mainly by haematopoietic cells, such as monocytes/ macrophages and lymphocytes[8]. Other cells, such as fibroblasts, endothelial cells, astrocytes and bone marrow stromal cells can also produce G-CSF following activation by lipopolysaccharide (LPS), IL-1 or TNF-α[1, 21, 26, 27]. Since serum G-CSF levels are rapidly elevated by bacterial products, G-CSF has a major role *in vivo* as host defence against microorganisms. In an "emergency" or "stress" situation, such as infection with pathogenic organisms, a component of a typical host response includes increased production of neutrophils for tissue restoration by eliminating invading organisms and removing damaged cells[1, 28].

I.3 Granulocyte-Colony Stimulating Factor Receptor

G-CSF mediates its biological actions by binding to a specific cell-surface receptor, the G-CSFR, a member of the hematopoietic cytokine receptor (HCR) super-family which forms homo-oligomeric complexes upon ligand binding to its extracellular surface[18]. As a member of the HCR super-family, G-CSFR possesses the characteristic features of a conserved WSXWS motif in the extracellular domain and the receptor

intracellular region does not contain any intrinsic enzymatic function[29]. The cytoplasmic region of the G-CSFR can be subdivided into a membrane-proximal domain, which contains two conserved sub-domains known as box 1 and box 2, and a membrane-distal domain, which contains a less conserved box 3 sequence[18]. In addition, there are four tyrosine residues in the cytoplasmic region of the G-CSFR at positions 704, 729, 744 and 764 of the human receptor, three of which lie in the membrane-distal domain[30]. Studies in cell lines have established that these conserved tyrosines (tyr704, tyr729, tyr744, tyr764) contribute significantly to G-CSF–induced proliferation, differentiation, and cell survival[31]. G-CSF binds to the external domain in a pocket formed by the N-terminal immunoglobulin domain and the cytokine receptor homology domain. Three fibronectin domains make up the rest of the external domain[29]. An important fact is the closeness between G-CSFR and gp130, a component of the IL-6 receptor complex[29], revealing that they possibly have a common evolutionary origin although they have evolved to perform different functions: induction of B-cell differentiation (IL-6) and stimulation of neutrophil proliferation (G-CSF)[32].

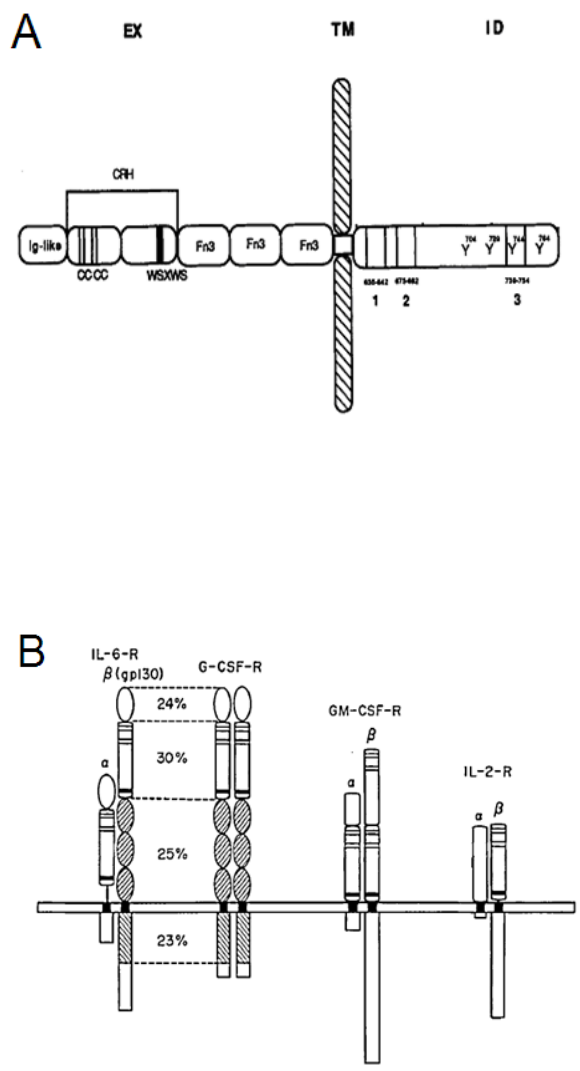

Fig. 2 – **A:** Schematic diagram of the structure of the human G-CSFR. The extracellular region (EX) of the G-CSFR contains an Ig-like domain, a cytokine receptor homologous region (CRH) with conserved cysteine (C) residues and the WSXWS motif, and three fibronectin type III (Fn3) domains. The intracellular domain (ID) of the G-CSFR contains three subdomains, designated boxes 1,2, and 3. Numbers correspond to amino acid residues. TM, transmembrane domain; Y, tyrosine residues[24].

B: Schematic representation of the homo- and hetero-dimeric structures of functional receptors for IL-6, G-CSF, GM-CSF and IL-2. The CRH domains containing the conserved cysteine residues (thin bars) and the WSXWS motif (thick bar) are indicated by shaded boxes. The gp130 (the β-chain of the IL-6 receptor) has a remarkable similarity to the G-CSFR. The numbers indicate the percentage of identical amino acids in each subdomain[23].

Both G-CSF and G-CSFR are present in nearly every organ in human fetal tissues[33]. G-CSFR has been shown to be expressed on myeloid progenitor cells, myeloid leukemia cells, leukemic cell lines, mature neutrophils, platelets, monocytes and some lymphoid cell lines[25]. In addition, G-CSFR has been detected on several non-hematopoietic cell types, including placenta trophoblastic cells and some lung carcinoma cell lines[34]. The physiological significance of G-CSFR on the surface of non-hematopoietic cells becomes more intriguing as more data comes to light. Bocchietto *et al.*[35] have shown that microvascular endothelial cells (EC) proliferate when stimulated with G-CSF, due to the activation of G-CSFR. Fuste and colleagues[36] have also shown that G-CSF increases the expression of adhesion receptors on EC, thus promoting leukocyte adhesion. This effect seems to be triggered by the signalling events that follow receptor binding and consequent activation of p38 MAPK, which is required to promote expression of adhesion receptors in endothelial cells. Most recently, Park *et al.*[37] have shown that G-CSF treatment significantly induced monocytes to produce IL-6, and culture supernatants of G-CSF-stimulated monocytes induced C-reactive protein (CRP) production in hepatocytes. On the other hand, in the same study G-CSF directly promoted EC proliferation and migration and could reverse the deleterious effects of CRP by activating the Akt/eNOS pathway. Harada and colleagues[38] have examined the presence of G-CSFR by immunoreactivity on adult mouse heart and cultured neonatal cardiomyocytes. They have shown G-CSFR localization in the cytoplasm and cell membrane under steady-state conditions, as it has been similarly reported in other living cells[39]. In addition to cardiomyocytes, this group also detected the expression of G-CSFR on cardiac fibroblasts.

I.4 Signalling pathways activated by G-CSF and its receptor

G-CSF is an essential growth factor for the optimal production of neutrophils and their precursors. When either G-CSF or its cognate receptor are genetically ablated, the resulting mice are severely neutropenic and susceptible to opportunistic infections[20, 40, 41]. The loss of G-CSF signalling accounts for the defects on proliferation, differentiation and survival at the progenitor, precursor or terminally differentiated neutrophil stages. The structural functional analysis of the G-CSFR attributes proliferative signalling to the proximal domain (~60 amino acids proximal to the plasma

membrane) and differentiation signalling to the distal domain (~100 amino acids at the C-terminus)[29].

Current models of cytokine receptor signalling, including that for G-CSFR, assign a critical signal transduction role to Janus kinases (Jak). Although Jak2-deficient mice display major defects in IL-3 and GM-CSF signalling, mice deficient in either Jak1 or Jak2 have intact G-CSFR signalling[42, 43]. The Src family of proto-oncogenic tyrosine kinases seems to have a more important role in transducing G-CSF-induced cell cycle progression. Since Src kinases have a wider range of physiological substrates than do the Jaks, which primarily affect the STAT proteins, Src kinases may play a more important role in G-CSF-mediated cell survival and metabolism. These pathways that involve Erk1/2 or PI3-kinase may contribute to G-CSF-induced proliferation, differentiation, survival and cytoskeletal reorganization[29]. Multiple protein tyrosine kinases (PTK) (e.g., Jak2 and Src) probably phosphorylate the tyrosine residues (tyr704, tyr729, tyr744 and tyr764) of the G-CSFR[44]. When phosphorylated, the phosphotyrosine residues serve as docking sites for signalling proteins containing phosphotyrosine binding domains (e.g., SH2 or PTB). Recruitment of these signalling proteins serves to diversify and inactivate G-CSFR signal. Diversification involves recruitment of the STAT transcription factors and Ras/Erk1/2 and PI3-kinase pathways (**Fig. 3**). Tyr704 can be phosphorylated by the Jaks and then serve as a docking site for the SH2 domains of STAT proteins[45]. Resembling that site, when phosphorylated, tyr729 may also serve as a docking site for the SH2 domain of STAT. Tyr764 favours the Src kinase and the Src SH2 domain[46]. This site is also the preferred binding site for the SH2 domains of Grb2 and is functionally coupled to Shc and the SH2-containing tyrosine phosphatise-2 (Shp-2)[47]. Grb2 also interacts with Gab2, which leads to PI3-kinase activity[48]. Tyr764 is also functionally coupled to Ras activation and Jun kinase[49]. Thus, phosphor-tyr764 can transduce several different signals, with both positive and negative effects on growth. Substrate availability and sustained activation may determine functional outcome. In their phosphorylated states, tyr 744 and tyr 729 may serve as docking sites for cytokine inducible SH2 protein/suppressor of cytokine signalling (SOCS) and SH2-containing inositol phosphatese (SHIP)[50]. Both molecules are negative regulators of Jak-STAT and PI3-kinase, respectively. The C-terminal domain also recruits SH2-containing tyrosine phosphatise-1 (Shp-1), which dephosphorylates positive signalling molecules such as Lyn and STAT[51]. According to what was said, while there may be a crosstalk between Src and Jak signalling pathways,

each kinase can trigger a stereotyped response, e.g., Jak-STAT and Src-Ras/Pi3-kinase[29].

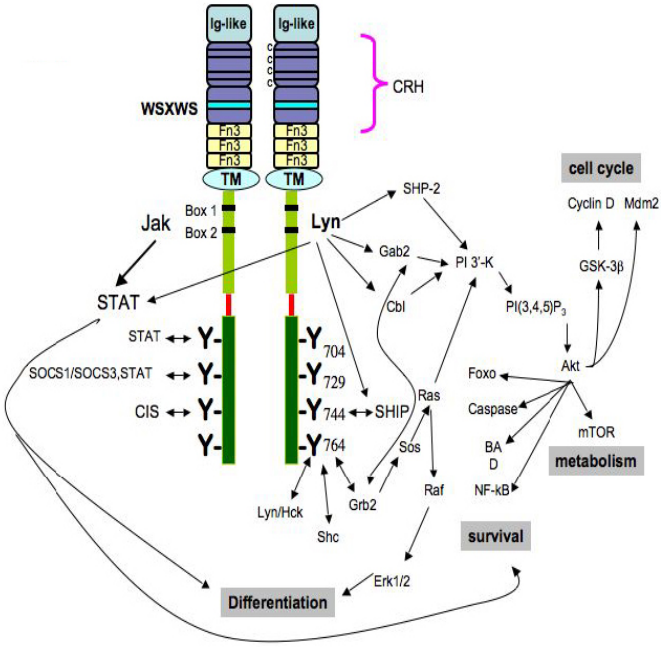

Fig. 3 – Diverse intracellular signalling pathways of the G-CSF Receptor. The cytoplasmic domain of the receptor contains Box 1 and Box 2 and Tyr704 in the proximal domain, necessary for mitogenesis. When phosphorylated, the four tyrosine residues serve as docking sites for SH2-containing proteins. Neither the structural basis of how cytosolic PTKs, such as Jak and Lyn, associate with the receptor, nor the specificity or redundancy of each tyrosine residue's kinase are known[28].

Proliferating responses are predominantly mediated by tyr704 and tyr764, with a minor contribution from tyr 744. The homodimerization of G-CSFR by ligand binding is associated with activation of Jak-STAT signalling pathways. Activated STATs translocate to the nucleus and induce gene transcription. It seems that STAT5 is a key player in proliferation signalling since inhibition of this signalling molecule is able to inhibit proliferation but not differentiation in a myeloid cell line[1]. **Survival and differentiation** signals are most strongly transduced by tyr704 and tyr744 leading to the activation of STAT3, suggesting that STAT3 activation may represent a key pathway in maturation signalling[52]. Heterogeneity in the signalling function of the G-CSFR is observed under different receptor saturation conditions that typically occur *in vivo*. Thus, during basal 'steady state' granulopoiesis, (low) G-CSF appears to trigger only a subset of signalling pathways involved in differentiation and survival (e.g. STAT3), whereas in 'emergency' conditions, such as bacterial infections (high G-CSF), proliferative pathways are also engaged (e.g. STAT5, Shc).

G-CSF primes neutrophils for pro-inflammatory responses and Src PTKs play a major role. According to Berton *et al.*[53], phagocytic cells from Src-deficient mice are defective in superoxide production, degranulation or migration. A major signalling pathway, which is Src-associated, is the one involving PI3-kinase. In this pathway

serine/threonine kinase Akt was identified as a downstream target. Zhu *et al.*[54] have shown that G-CSF stimulation of granulocytes displayed a time- and dose-dependent increase in reactive oxygen species (ROS) production, which was correlated with activation of Lyn and Akt. According to these authors, inhibition of Lyn, PI3-kinase, Akt or NADPH oxidase abrogated G-CSF-induced ROS production. It was also shown by this group that G-CSF induces serine phosphorylation and membrane translocation of p47phox, a subunit of NADPH oxidase and an essential step to the activation of this enzyme system. These data support the finding that G-CSF induces ROS production in neutrophils via NADPH oxidase and phosphorylation of p47phox by Akt.

I.5 Neutrophils and Reactive Oxygen Species (ROS)

Neutrophil granulocytes (a.k.a., polymorphonuclear leukocytes) are normally found circulating in the bloodstream (half-life of ≅7 h) and migrating through tissues (2–3 days), devoting their short lifetime to surveillance[55]. During an infection, the neutrophil lifespan is increased, and large numbers of neutrophils are rapidly recruited to the site(s) of infection where they function to destroy invading pathogens. In this manner, neutrophils serve as one of the body's first lines of defence against infection. These cells use an extraordinary array of oxygen-dependent and oxygen-independent microbicidal weapons to destroy and remove infectious agents[56]. Oxygen-dependent mechanisms involve the production of ROS, which can be microbicidal[57], and oxygen-independent mechanisms include most other neutrophil functions, such as chemotaxis, phagocytosis, degranulation, and release of lytic enzymes and bactericidal peptides[56]. ROS are oxygen-derived small molecules, including oxygen radicals [superoxide ($O_2^{\bullet-}$), hydroxyl ($^{\bullet}OH$), peroxyl ($RO_2^{\bullet}$), and alkoxyl ($RO^{\bullet}$) radicals] and certain non-radicals that are either oxidizing agents and/or are easily converted into radicals, such as hypochlorous acid (HOCl), ozone (O_3), singlet oxygen ($^1O_2$), and hydrogen peroxide (H_2O_2). ROS generation is generally a cascade of reactions that starts with the production of superoxide. Superoxide rapidly dismutates to hydrogen peroxide either spontaneously (at low pH) or catalyzed by superoxide dismutase (SOD). Other elements in the cascade of ROS generation include the reaction of superoxide with nitric oxide to form peroxynitrite ($ONOO^-$), the peroxidase-catalyzed formation of hypochlorous acid

(HOCl) from hydrogen peroxide, and the iron-catalyzed Fenton reaction leading to the generation of hydroxyl radical[58]. ROS avidly interact with a large number of molecules including other small inorganic molecules as well as proteins, lipids, carbohydrates, and nucleic acids. Through such interactions, ROS may irreversibly destroy or alter the function of the target molecule and consequently, ROS have been increasingly identified as major contributors to damage in biological organisms. However, ROS are involved not only in cellular damage and killing of pathogens, but also in a large number of reversible regulatory signalling processes in virtually all cells and tissues[59]. The physiological generation of ROS can occur as a result of other biological reactions. For example, ROS generation occurs as a byproduct in the mitochondria, peroxisomes, cytochrome *P*-450, and other cellular elements[58]. The phagocyte NADPH oxidase was the first identified example of a system that generates ROS not as a byproduct, but rather as the primary function of this enzyme system[59].

I.6 NADPH oxidase

In general, the best characterized plasma membrane oxidase is the phagocytic NADPH oxidase, a multicomponent enzyme composed of four oxidase-specific proteins (p22*phox*, p47*phox*, p67*phox*, and gp91*phox*) and a GTPase (Rac1/2). One other oxidase-specific protein (p40*phox*) and a second GTPase (Rap1A) have also been shown to play roles in regulating oxidase activity; however, their specific functions are still not well understood[60]. Originally, the nomenclature for the various components differed throughout the literature (**Table 1**); however, the generally accepted nomenclature for the phagocyte oxidase specific components now includes the suffix *phox*, which refers to *ph*agocyte *ox*idase[61]. The only one exception is gp91*phox*, which has also been named NADPH oxidase 2 (Nox2)[62].

A

	Other Names	Chromosome Location	Gene Length	Amino Acids	Total SNP
NOX1	NOH-1, MOX1, GP91-2	Xq22	30374	564	79
NOX2	CYBB, gp91^{phox}	Xp21.1	33451	570	69
NOX3	GP91-3	6q25.1-26	60534	568	228
NOX4	RENOX, KOX-1, KOX	11q14.2-q21	165139	578	858
NOX5		15q22.31	42392	747	263
DUOX1	Thox1, LNOX1, NOXEF1	15q21	35583	1,551	188
DUOX2	Thox2, LNOX2, NOXEF2, p138^{lox}	15q15.3-q21	20757	1,548	188
p22^{phox}	CYBA	16q24	9486	195	117
p47^{phox}	NOXO2, NCF1, NCF47K	7q11.23	15349	390	76
NOXO1	p41NOX	16p13.3	2522	370	13
p67^{phox}	NOXA2, NCF2	1q25	34845	526	125
NOXA1	p51NOX	9q34.3	11011	483	38
p40^{phox}	NCF4	22q1,3.1	17028	339	100

B

	High-Level Expression	Intermediate- to Low-Level Expression
NOX1	Colon	Smooth muscle, endothelium, uterus, placenta, prostate, osteoclasts, retinal pericytes
NOX2	Phagocytes	B lymphocytes, neurons, cardiomyocytes, skeletal muscle, hepatocytes, endothelium, hematopoietic stem cells, smooth muscle
NOX3	Inner ear	Fetal kidney, fetal spleen, skull bone, brain
NOX4	Kidney, blood vessels	Osteoclasts, endothelium, smooth muscle, hematopoietic stem cells, fibroblasts, keratinocytes, melanoma cells, neurons
NOX5	Lymphoid tissue, testis	Endothelium, smooth muscle, pancreas, placenta, ovary, uterus, stomach, various fetal tissues
DUOX1	Thyroid	Airway epithelia, tongue epithelium, cerebellum, testis
DUOX2	Thyroid	Salivary and rectal glands, gastrointestinal epithelia, airway epithelia, uterus, gall bladder, pancreatic islets

Table 1 – **A:** Nox enzymes and subunits: alternative names, chromosomal localization, gene length, number of amino acids, and total number of single-nucleotide polymorphisms (total SNP). **B:** Tissue distribution of Nox enzymes: Nox enzymes are expressed in a small number of tissues at high levels (readily detected by Northern blotting) but show intermediate- to low-level expression in many other tissues[57].

Increasing evidence at both message and protein level suggests that Nox2 is among the most widely distributed NADPH oxidase isoforms, being reported to be expressed inclusively in normal human cardiomyocytes. Krijnen *et al.*[63] revealed in their study that in patients with acute myocardial infarction (AMI), there was a significant increase in Nox2 expression, both in viable and in jeopardised cardiomyocytes, in the infarcted area. The activation of Nox2 occurs through a complex series of protein/protein interactions, where Nox2 constitutively associates with p22phox, forming a heterodimeric complex known as cytochrome *b*558 (Cyt *b*558)[58]. NADPH oxidase activation requires translocation of cytosolic factors to the Nox2/p22phox complex and the present working model functions in the following way (**Fig. 4**): First, phosphorylation of p47phox leads to a conformational change allowing its interaction with p22phox. It is thought that p47phox organizes the translocation of other cytosolic factors, hence its designation as "organizer subunit." The relocalization of p47phox to the membrane brings the "activator subunit" p67phox into contact with Nox2 and also brings the small subunit p40phox to the complex. Finally, the GTPase Rac interacts with Nox2 via a two-step mechanism involving an initial direct interaction with Nox2, followed by a subsequent interaction with p67phox. Once assembled, the complex is active and generates superoxide by transferring an electron from NADPH in the cytosol to oxygen on the luminal or extracellular space[59].

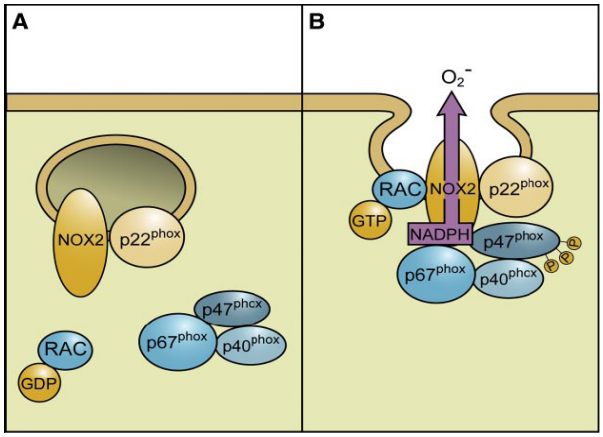

Fig. 4 - Assembly of the phagocyte NADPH oxidase Nox2. Nox2 and p22phox are found primarily in the membrane of intracellular vesicles. Upon activation, there is an exchange of GDP for GTP on Rac leading to its activation. Phosphorylation of the cytosolic p47phox subunit leads to conformational changes allowing interaction with p22phox. The movement of p47phox brings with it the other cytoplasmic subunits, p67phox and p40phox, to form the active Nox2 enzyme complex. Once activated, there is a fusion of Nox2-containing vesicles with the plasma membrane or the phagosomal membrane. The active enzyme complex transports electrons from cytoplasmic NADPH to extracellular or phagosomal oxygen to generate superoxide[57].

I.7 G-CSF role on myocardial protection

G-CSF is known as a neovascularization promoter by stimulating vascular endothelial growth factor (VEGF) secretion in neutrophils. Ohki *et al.*[64] have shown the ability of G-CSF to improve the VEGF production per neutrophil above the levels seen in a steady state. Concurrent with augmented neutrophil counts, mice plasma VEGF levels increase after G-CSF treatment, reaching a peak level after 5 days of treatment. By using a model of hindlimb ischemia, this group has shown that blood flow in the ischemic limb recovered faster in the G-CSF-treated group compared with controls. With co-injection of neutralizing antibodies against either VEGF receptor 1 (VEGFR1) and/or VEGFR2, they were able to conclude that G-CSF-mediated angiogenesis was promoted by a major co-recruitment of VEGFR1 in neutrophils.

Bone marrow stem cells (BMSCs) have been appraised for some years as a potential tool in regenerative medicine. In 2001, Orlic *et al.*[65] have demonstrated that BMSCs could differentiate into cardiac myocytes, ECs and vascular smooth muscle cells (VSMCs) in an adult mouse model of AMI. Within 5h after ligation of the left coronary artery in adult female mice, they injected male BMSCs (Lin^- $c\text{-}kit^+$) that carried a gene encoding an enhanced green fluorescent protein (eGFP), which was delivered into the myocardium near the site of infarction. After 9 days, the regeneration of the myocardium was observed. These regenerative regions consisted of Y-positive $eGFP^+$ cardiac myocytes and small coronary vessels. Regeneration of the myocardium was not recognized in hearts that were injected Lin^- $c\text{-}kit^-$ bone marrow cells which are conceived to be devoid of stem cells. This suggested that hematopoietic stem cells (HSCs), as opposed to other bone marrow resident cells, were responsible for the regeneration of myocardium. Furthermore, they examined whether cytokine treatment increases BMSCs mobilization to the injured myocardium and promotes myocardial regeneration[66]. After mice were injected with rat stem cell factor (SCF) and recombinant human G-CSF for 5 days, the animals were subjected to ligation of the left coronary artery. SCF and G-CSF were given for 3 more days after the ligation of the artery. Cytokine-mediated mobilization of BMSCs resulted in myocardial regeneration, characterized by dividing cardiac myocytes and the formation of vascular structures 27 days after AMI. This method significantly improved cardiac function assessed by ejection fraction, left ventricle (LV) diameter and LV pressure. Although their results suggest that locally delivered BMSCs could generate new myocardium and then

improve the prognosis of patients with AMI, recent studies have demonstrated that adult HSCs do not transdifferentiate into cardiac myocytes in the murine AMI model[67, 68].

Iwanaga *et al.*[69] have examined whether G-CSF treatment would be effective in preventing cardiac remodelling after myocardial infarction (MI) in large animals. By producing a ligation of the left anterior descending coronary artery in swine and sub-cutaneously administrating G-CSF during the following days, they have shown an improved cardiac function and reduced LV remodelling. By analysing the ischemic region, they've seen a smaller number of apoptotic ECs and a larger number of vessels in the G-CSF treated group in comparison with the controls. Moreover, in the G-CSF-treated group, VEGF was more abundantly expressed and Akt more strongly activated in the ischemic region. Since Akt has been reported to play a role in cell survival and angiogenesis, they extrapolated that Akt could be important for the cardioprotective effects of G-CSF. A fact that caught these investigators' attention was the difference in LV function between the G-CSF treatment group and the controls, seen already one week after AMI. They speculated that this finding was not simply explained by G-CSF-induced mobilization of BMSCs into the injured myocardium, but that G-CSF could also have direct actions on the myocardium in the setting of AMI. At this point it had been reported that G-CSFR was expressed on various blood cells, but whether it was expressed on cardiomyocytes was still in doubt. With this in mind, the same group of investigators decided to analyse the expression of G-CSFR messenger ribonucleic acid (mRNA) in both adult mouse heart and in cultured neonatal mouse cardiomyocytes by reverse transcription-polymerase reaction (RT-PCR), confirming that G-CSFR was expressed in cardiomyocytes and thereby possible direct effects of G-CSF on the myocardium[38]. In cultured cardiomyocytes, they also have shown a G-CSF-activation of intracellular molecules like Jak2, STAT-1 and STAT-3 in a dose-dependent manner. Next, they further examined whether G-CSF would have a direct effect on the myocardium after ischemia-reperfusion injury by using a Langendorff-perfused heart model[70]. The isolated hearts underwent 35 min-ischemia followed by 120-min reperfusion with a perfusate containing G-CSF or vehicle. G-CSF significantly reduced the infarct size and strongly activated Jak2, STAT3, Akt and endothelial NO synthase (eNOS) in the hearts subjected to ischemia-reperfusion. The G-CSF-induced reduction in infarct size was abolished by inhibitors of PI3-kinase, Jak2 and NOS. Since in this experimental model there are no blood cells nor inflammatory mediators, G-CSF effects were regarded as direct effects on the myocardium during ischemia-reperfusion injury

and it was assumed that cardioprotective effects of G-CSF were mediated through the Akt-endothelial NOS pathway.

It is still unclear whether G-CSF exerts positive or negative effects on the progression of atherosclerosis. Haghighat *et al*.[71] were the first group to investigate the effect of short-term administration of G-CSF or GM-CSF on atherosclerotic plaque progression in a murine model of atherosclerosis. The study revealed that when combined with high-fat diet, both G-CSF and GM-CSF accelerated the formation of atherosclerotic lesions in Apo $E^{-/-}$ mice, rather than ameliorating the extent of lesions. Surprisingly, these effects could not be explained with any consistent changes in hemodynamics, local inflammation, lipid profiles or systemic inflammation that could provide a plausible explanation for the striking effects of G-CSF and GM-CSF treatment on atherosclerotic lesions. A potential reason for the deleterious effects of the cytokines was the induction of neovascularization in the arterial wall, which was markedly increased with GM-CSF or G-CSF treatments in comparison with controls. Previously, the association that coronary vasa vasorum neovascularization precedes the development of endothelial dysfunction and atherosclerotic development had already been made[72, 73]. Although the study by Haghighat *et al.*[71] clearly demonstrate an association between G-CSF and GM-CSF-enhanced atherosclerosis and neovascularization in the arterial wall, causality has not yet been proven.

Chapter II: **Mechanisms of vascular growth**

When Leonardo da Vinci first speculated about the heart and the circulatory system, he could only analyse the mechanism of organ formation by analogy. So he suggested that the vasculature developed like a tree from a seed (the heart) by sprouting roots (the liver capillary network) and a trunk with major branches (the aorta and arteries, **Fig. 5**).

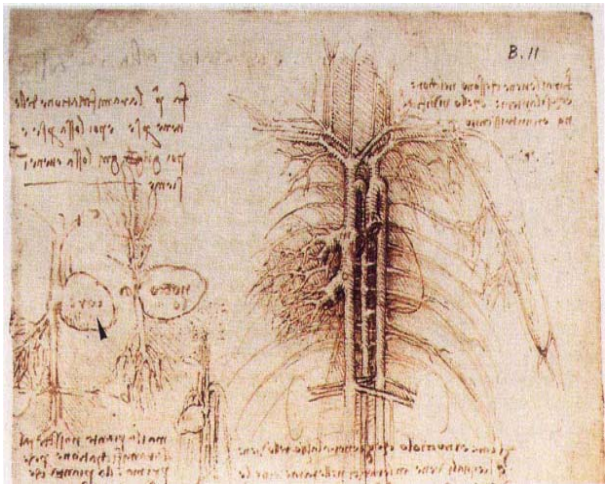

Fig. 5 – Analogy between the botanic and vascular tree as drawn by Leonardo da Vinci (taken from "The anatomy of man: the cardiovascular system (1508)). The drawing is annotated in his cryptic mirror-writing, for example the big seed of the left plant labelled "core" (heart) is indicated by the arrowhead [71].

Although sprouting of vessels is indeed a principal mechanism of the blood vessel formation termed angiogenesis, other mechanisms are now known. Rather than sprouting from the heart, the vascular system is laid down before the heart starts beating. Conversely, adult blood vessels generally form from pre-existing vessels in direct response to tissue demands[74].

II.1 Vasculogenesis and Angiogenesis

The early vascular plexus forms from the mesoderm by differentiation of angioblasts (vascular endothelial cells that have not yet formed a lumen), which subsequently generate primitive blood vessels. The molecular mechanisms responsible for this process, termed **vasculogenesis**[74], are starting to emerge (**Fig. 6**).

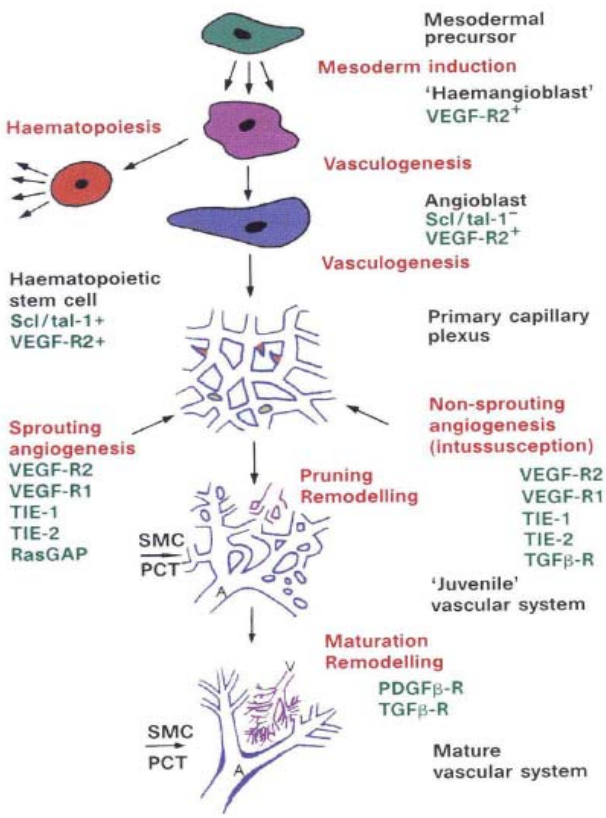

Fig. 6 – The processes (red labels), molecules (green labels) and appearances (black labels) involved in vascular development. Red tips in the primary capillary plexus represent sprouts, yellow circles represent splitting pillars. The hemangioblast as a bipotential precursor is still under debate and intermediate steps between some processes have been omitted. Remodelling and maturation is dependent on the tissue and organ context. It is schematized here from observations in the avian yolk-sac vascular system. A, arteriole; V, venule; SMC, smoothe muscle cells; PCT, pericytes[71].

Mesoderm inducing factors of the fibroblast growth factor family are crucial in inducing paraxial and lateral plate mesoderm to form angioblasts and hematopoietic cells. The existence of a bipotential precursor of these cell types (the so-called hemangioblast) is suggested by defects in both the hematopoietic and angioblastic lineages of embryos lacking VEGF-receptor 2 (VEGF-R2, also called Flk-1 and KDR in mice and humans, respectively). After differentiation, VEGF-R2 is downregulated in hematopoietic but not in endothelial cells. The other receptor for VEGF, VEGF-R1 (Flt-1), plays a later role, as mice lacking VEGF-R1 produce angioblasts, but their assembly into functional blood vessels is impaired[75]. VEGF acts in a paracrine manner as it is produced by the endoderm, whereas its receptors are expressed by mesoderm-derived angioblasts. Some angioblasts can migrate over long distances and form a vascular plexus at a site distant from the original location[74].

After the primary plexus is formed, more ECs are generated, which can form new capillaries by sprouting or by splitting from their vessel of origin in a process termed **angiogenesis**. There are at least two different types of angiogenesis: 1) non-sprouting or intussusception angiogenesis and 2) true sprouting of capillaries from pre-existing vessels (**Fig. 7**)[74]. In general, the first process involves the enlargement of venules, which become divided by pillars of periendothelial cells (intussusceptions) or

by transendothelial cell bridges, which then split into individual capillaries[76]. In sprouting angiogenesis, endothelial cells proliferate behind the tip cell of a growing branch in response to cytokines, such as VEGF, and lumens can form by vacuole fusion. Both forms of angiogenesis require the recruitment of smooth muscle cells (SMCs) to stabilize the nascent vessels.

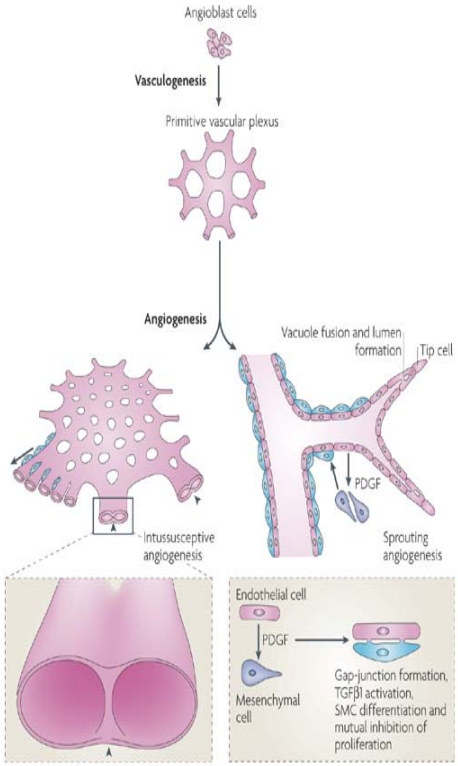

Fig. 7 – Representation of vasculogenesis and two types of angiogenesis: intussusceptive and sprouting angiogenesis. Vasculogenesis involves the differentiation of endothelial cells (ECs) from precursor angioblast cells to form a primitive plexus of capillaries, which remodel and grow by angiogenesis. Intussusceptive angiogenesis involves the splitting and growing of vessels *in situ*. Vessel splitting occurs by the formation of translumen pillars (arrowheads) but the molecular mechanisms are not well understood[74].

The nascent vascular bed expands by sprouting and matures into a system of stable vessels. Angiogenesis is a complex process, involving multiple gene products expressed by different cell types, all contributing to an integrated sequence of events[76]. Hypoxia is an important stimulus for expansion of vascular bed. Initially, cells are oxygenated by simple diffusion of oxygen, but when tissues grow beyond the limit of oxygen diffusion, hypoxia triggers vessel growth by signalling through hypoxia-inducible transcription factors (HIFs)[76]. A large number of genes involved in different steps of angiogenesis are independently responsive to hypoxia. Examples include nitric oxide synthases (involved in governing vascular tone), growth factors such as VEGF - which becomes up-regulated by 30-fold within minutes, angiopoietins (Ang-1 and Ang-2), fibroblast growth factors and their various receptors, and genes involved in matrix metabolism, including matrix metalloproteinases, plasminogen activator receptors and inhibitors, and collagen prolyl hydroxilase[77, 78, 79, 74]. Establishment of a functional

vascular network further requires that nascent vessels mature into durable vessels. The association of pericytes and SMCs with newly formed vessels regulates EC proliferation, survival, migration, differentiation, vascular branching, blood flow and vascular permeability. Platelet-derived growth factor (PDGF) and its receptor have essential roles in the stabilization of nascent blood vessels by recruitment of mesenchymal progenitors[76]. Neighbouring mesenchymal cells migrate towards the new vessel in response to PDGF and then differentiate into vascular SMCs (vSMCs) in response to TGF-β signalling[80].

II.2 Coronary Collateral Growth (CCG)

Unlike distal capillaries, which distribute blood flow to individual cells, arteries provide bulk flow to the tissue. Under normal conditions myocardial blood flow is routed through the major coronary arterial branches and then to the different regions of the myocardium via a series of side branches, terminating in an extensive capillary network. When one of the major conduits is obstructed by an atherosclerotic lesion, flow to the injury is interrupted. Whether the tissue distal to the obstruction goes on to ischemic necrosis or retains its functional and structural integrity depends on the adequacy of flow reaching it via alternate anastomotic channels. The anastomotic collateral communications have been the subject of many investigations since the 1920s and were later separated by Bloor and Liebow[81] into four types: endomural, retrocardiac, transepicardial and intracoronary. Of the referred groups, the one receiving the most attention has been the intracoronary collaterals, that is, the anastomosing branches between adjacent primary coronary arteries[82]. **Coronary collaterals**, or "natural bypasses," are anastomotic connections without an interposed capillary bed either between portions of the same coronary artery or between different coronary arteries[83], potentially offering an important alternative source of blood supply when the original vessel fails to provide sufficient blood[84]. **Collateral growth** (commonly termed *arteriogenesis*) refers to the transformation of pre-existing (collateral) arterioles into functional (muscular) collateral arteries, as a thick muscular coat is added, concomitant with the acquisition of viscoelastic and vasomotor properties[76]. Under normal conditions, in the absence of pathology, there is little to no net blood flow through these collateral anastomoses. In their innate, native state, collateral vessels are very small and

sparse in number (small total cross-sectional area), promoting high resistance to net blood flow, and their existence appears to have little purpose. However, if challenged with an appropriate stimulus, collaterals can greatly expand their calibre and serve as conduits that bear little resistance to blood flow. Collateral growth is a remodelling process that represents organized abluminal expansion of pre-existing vessels (**Fig. 8**), involving mitosis of endothelial, smooth muscle, and likely other vascular cells (e.g., fibroblasts). Since this adaptive mechanism could considerably confine the effects of vascular pathology, individuals who can develop collaterals would be better fit to circumvent the effects of an acute vascular injury[85].

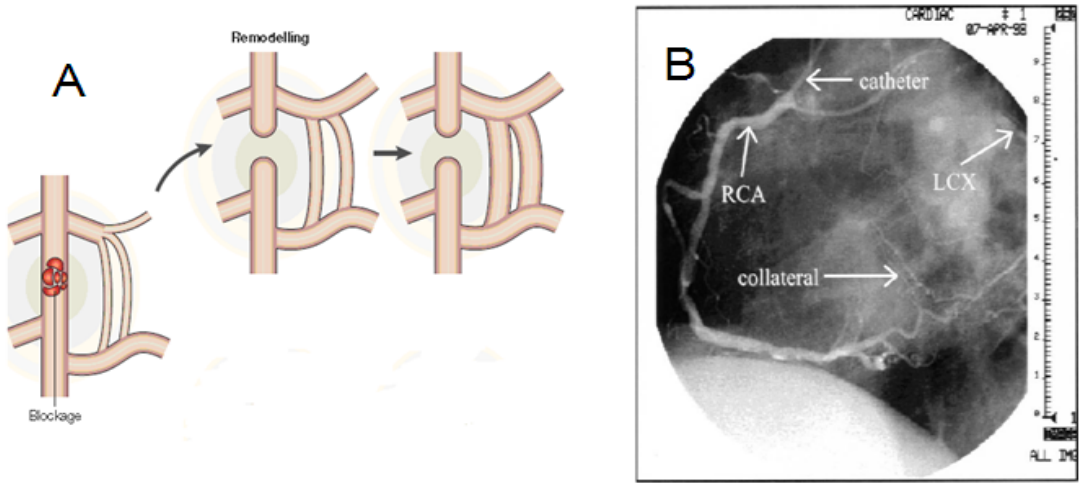

Fig. 8 – **A:** Collateral vessels can develop around the site of coronary occlusion, via remodelling of pre-existing vessels (arteriogenesis) that gradually enlarge to the point at which they can carry the bulk of blood flow[84].
B: Left anterior oblique view of the right coronary arteriogram. The left circumflex coronary artery (LCX) is proximally occluded and fills completely by means of collateral circulation from the right coronary artery (RCA)[81].

II.3 Controversies on CCG

While the development of vasculature in the course of embryonic growth is beginning to be well understood, comparatively little information is available about the processes responsible for coronary collateral growth. There is still much debate on which causal factors initiate collateral growth. Two hypotheses are on the discussion table: one hypothesis claims that shear stress is the initiating factor[86], while the other

suggests that ischemia initiates collateral growth[87]. In order to fully understand both arguments, it is important to recognize the differences in each organ's anatomical features, which may provide insight on the factors responsible for growth. The comparison between the development of collateral vessels in skeletal muscle versus in the heart illustrates the basis of the discussion. In coronary artery occlusion, the ischemic zone is adjacent to, and even interdigitating with, the normally perfused zone of the myocardium. Thus, the ischemic area of the heart is relatively close to the area where collateral growth occurs. In contrast, after occlusion of a femoral artery, the source of ischemia is located in the region of the groin, but the level of ischemia is most intense in the toes – an area far away from the site of vascular growth. Accordingly, collateral growth in different organ systems may be stimulated by a unique conjunction of factors, which is ultimately related to the anatomical relations between the site of vascular growth and the site of ischemia[85]. However, there is still not a complete understanding of how vascular communication functions between remote tissue areas. Birnbaum *et al.* have shown that remote ischemia of a skeletal muscle, induced by muscle stimulation combined with restriction of blood flow, preconditioned the myocardium and reduced myocardial infarction size considerably[88]. In other studies, Verdouw and colleagues conclude that a number of distinctly different stimuli can protect the myocardium, suggesting that ischemic myocardial preconditioning could be just one feature of a more general protection phenomenon[89, 90]. These observations show us that even though the zone of ischemia is far away from the site of growth, this does not mean that ischemia is not involved in triggering a protective response.

The role of shear stress in collateral growth has been discussed extensively by Wolfgang Schaper's research group and others[91, 92]. Their model is based on the following concept (**Fig. 9**): After occlusion of an artery, the pressure in its distal stump falls to very low levels. When a vascular connection like a pre-existent collateral anastomoses exists between the high-pressure (proximal to the occlusion) and the low pressure (distal from the occlusion) region, a steep pressure gradient develops which increases blood flow through these connections.

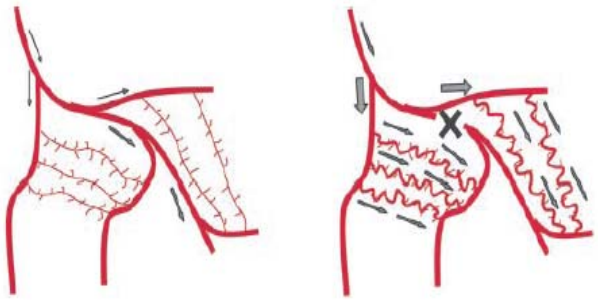

Fig. 9 – Diagram of blood flow changes after occlusion of the femoral artery in the rabbit hind limb. After occlusion of the femoral artery (X), blood flow (arrows) follows the gradient between pressures proximal to the occlusion site and very low distal pressures, recruting pre-existing collateral arterioles[89].

According to Heil and Schaper[91], the vessel wall is now exposed to pronounced mechanical forces: increased blood flow directly augments fluid shear stress (FSS), i.e., the viscous drag that flowing blood exerts on the endothelial lining. By assuming Newtonian fluid dynamics, FSS can be estimated using the following equation:

$$\tau = \frac{4\eta Q}{\pi R^3}$$

τ = fluid shear stress
η = blood viscosity
R = internal radius of vessel
Q = blood flow velocity

The authors demonstrate that blood flow (Q) will directly result in increased FSS (τ). The wall of the collateral arteriole is influenced by pressure-related forces like longitudinal-, circumferential- and radial-wall stresses. The distension of the vessel wall, structurally weakened by intravascular pressure, increases the circumferential wall stress (CWS). FSS is a relatively weak force compared with CWS, which is 10^6 times higher, posing the hypothesis that FSS can only act in concert with pressure-dependent forces[91]. With that in mind, Schaper's group created an arteriovenous shunt downstream of the collaterals (designed to increase flow and shear stress in the collaterals). However, that interposition of such a shunt would also worsen downstream ischemia, i.e., collateral-dependent flow that normally would perfuse the tissue at risk, is now shunted into the venous system. Thus, this experiment is not a definitive test for FSS because it does not exclude the effects of ischemia[85]. Another study performed by

Chilian and colleagues[87], attempted to resolve the contributions of FSS from those of ischemia to the coronary circulation by distally embolizing the microcirculation of the heart with microspheres, thus producing ischemia without pressure gradients across upstream collaterals. They observed initiation of collateral growth, but collateral growth was not nearly as robust as with other models. Thus, at least in the heart, ischemia can be thought of as an initiating factor, but shear stress is likely a factor that contributes to remodelling during the continuation of this process. Although FSS has been accepted by many as the factor that drives this process, the investigators concluding a role of shear stress in collateral growth have not measured shear stress itself[85]. According to Heil and Schaper[91], the influence of FSS on collateral growth although highly suggestive has remained conjectural and the evidence for it correlative, especially because FSS is almost impossible to measure in small collaterals.

Nowadays, there are several observations indicating that the process of collateral growth is likely a combination of multiple factors. Matsunaga *et al.*[93] observed that VEGF expression during coronary collateralization is time-dependent, i.e., maximum production occurs early during repetitive ischemia and then wanes as collateral growth progresses and ischemia decreases. Since VEGF has a HIF (hypoxia-inducible factor) element in its promoter[94], the idea that the early initiation of collateral growth is regulated by ischemia (and tissue hypoxia) gains more consistency. But, as collaterals develop and tissue hypoxia is ameliorated, the process of growth and enlargement continues. We could think that FSS could be a sustaining force after the VEGF signal wanes, but, according to Heil and Schaper[91] as soon as the collaterals start developing, pressure differences between high and low pressure regions also diminish and FSS becomes an irrelevant force. Another interesting fact to add to this equation of a multifactorial hypothesis for collateral growth was brought to light again by Matsunaga and his collaborators[95]. They observed that both VEGF and Angiopoietin-2 (Ang-2) expression in myocardial interstitial fluid waned after 3 days of repetitive occlusion. In contrast, the expression of Ang-1 remained relatively constant at all times, contributing to blood vessel maturation and stability. This reveals that, in the case of coronary collateral growth, there is a coordination of several growth factors. Another point worth emphasizing was the demonstration by Toyota *et al.*[96], that the neutralization of VEGF by antibodies prevented coronary collateral growth. This illustrates the importance of growth factors resultant from ischemic tissue and if the actions of growth factors are prevented, it appears, at least in the heart, collateral growth does not occur[85].

II.4 Redox-dependent signalling in CCG

Free radicals and ROS have been implicated in a large number of cardiovascular pathologies, like atherosclerosis and ischemia-reperfusion injury[97]. An excessive production or decreased scavenging of ROS leads to unbalanced physiological functions resulting in pathological states. As explained in the previous chapter, ROS include oxygen ions (O_2^-), free radicals [superoxide ($O_2^{\bullet -}$), hydroxyl radical ($^{\bullet}OH$)] and peroxides (hydrogen peroxide, H_2O_2). They are byproducts of normal metabolic processes of oxygen consumption in the body[58, 59]. ROS are small and highly reactive molecules with important cell signalling roles when maintained at proper cellular concentrations. Because of their highly reactive nature, ROS avidly interact with a large number of molecules and can modify other oxygen species, proteins and lipids, a situation often termed **oxidative stress**[98]. Through such interactions, ROS may irreversibly destroy or alter the function of the target molecule and consequently, ROS have been identified as major contributors to damage in biological organisms. However, there is a growing consensus that low levels of ROS play pivotal roles in neovascularization and myocardial adaptations to ischemia, including coronary collateral growth[85]. Components of angiogenesis include cell survival, proliferation and migration, all processes where ROS have been shown to perform a regulatory role. Yamaoka-Tojo *et al.*[99] have shown that ROS derived from NADPH oxidase mediate VEGF signalling, promoting EC migration and proliferation. Soon after, Tojo and colleagues[100] have demonstrated that gp91phox$^{-/-}$ mice have a diminished blood flow recovery and capillary density after ischemia, revealing that gp91phox-derived ROS play an important role in mediating neovascularization in ischemic tissue. In **Fig. 10**, Ushio-Fukai describes important ROS-dependent genes and proteins associated with anigiogenesis, like urokinase plasminogen activator (uPA), plasminogen activator inhibitor-1 (PAI-1) and metalloproteinases (MMPs). On the other hand, there was also impaired angiogenesis demonstrated in diseases characterized by elevated oxidative stress, including diabetes and hypertension[101, 102].

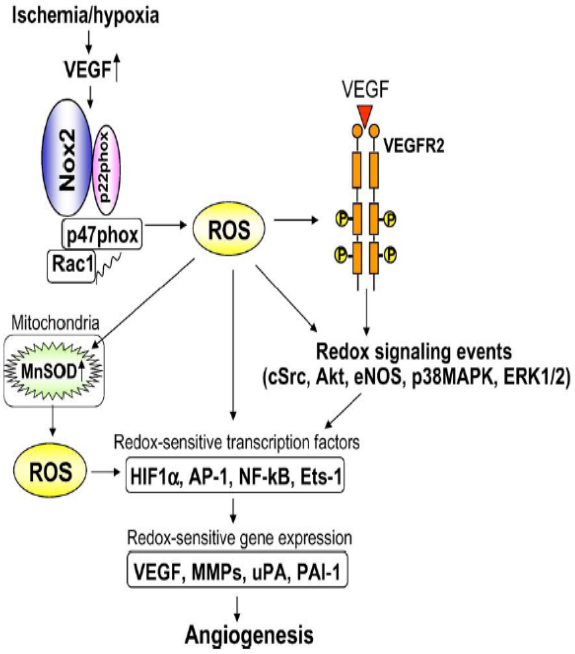

Fig. 10 - Role of ROS derived from NADPH oxidase in the induction of transcription factors and genes involved in angiogenesis. Ischemia/hypoxia stimulates VEGF induction and NADPH oxidase, thereby promoting activation of redox signalling events and induction of redox sensitive transcription factors and genes involved in angiogenesis. ROS derived from NADPH oxidase also upregulate mitochondrial SOD (MnSOD), increasing mitochondrial H_2O_2 production, which could represent a feed-forward mechanism by which ROS-triggered H_2O_2 formation plays an important role in angiogenesis[101].

In the setting of myocardial adaptations to ischemia, ROS can also have both positive and negative effects. **Ischemia-reperfusion injury**, the biphasic process characterized by exposure to prolonged reductions in blood flow (ischemia), elicits a variety of events that initiate cell death, promoted by a significant superoxide generation that occurs during ischemia before reperfusion[103]. Afterwards, due to damage of the electron transport chain in the mitochondria, massive amounts of ROS are released during reperfusion and cause myocardial tissue death by lipid peroxidation, protein modification and DNA damage[104-106]. On the contrary, **ischemic preconditioning** (IPC), a situation characterized by pre-exposure of the heart to a mild stress, like short periods of ischemia followed by reperfusion, has been shown to reduce cardiac damage from subsequent ischemic insults[107, 37]. Tissue such as the myocardium can be adapted to ischemic stress by repeatedly subjecting it to short terms of reversible ischemia, each followed by another short duration of reperfusion[108, 109]. This phenomenon causes the production of oxidative stress, leading to the induction of gene expression, which is subsequently translated into the development of beneficial proteins responsible for the heart's defence[97]. In 1995, Chen and colleagues[110] reported that a redox-based mechanism promoted cardioprotection during ischemic preconditioning. It was later found that the generation of ROS was a result of the opening of mitochondrial ATP-sensitive potassium channels (mKATP), acting as second messengers in a pathway that

ended in the activation of protein kinase C (PKC), which would then trigger the preconditioned state[111]. In those studies, ROS were recognized as part of the trigger pathway that preconditions the heart prior to the onset of ischemia. It was discovered that IPC actually exerts its protective effect in the first minutes of reperfusion[112], presumably by inhibiting the formation of mitochondrial permeability transition pores (mPTP)[113]. It was also found that redox signalling is part of the pathway that mediates IPC protection at the time of reperfusion, meaning that ROS generation was required for IPC to be protective[114]. It is unknown how redox signalling acts to mediate protection at reperfusion[115], but a number of signal transduction components have been identified in IPC's mediator pathway, including phosphatidylinositol (PI) 3-kinase and extracellular signal-regulated kinase (ERK)[112]. IPC was also shown to be at least partially dependent on Nox2, since ischemic preconditioning is completely abolished in Nox2-deficient mice[116], although the mechanism has not yet been fully elucidated.

Depletion of ROS impairs cell responses to mitogenic stimulation, and it is known that ROS can enhance the proliferation of vascular smooth muscle (VSMC) and endothelial cells (EC), which are primary features in the process of coronary collateralization[117, 118, 119, 120]. In 2007, Rocic *et al.*[121] have shown that a specific concentration range of superoxide is required for coronary collateral development and that elevated superoxide levels are detrimental for the process. Their results implicate that superoxide derived from flavin-containing oxidases is critical for coronary collateral growth, because diphenyleneiodonium (DPI), an inhibitor of nitric oxide synthase, blocked this process in response to ischemia-reperfusion *in vivo*. It was also shown in this work that inhibition of NADPH oxidases by apocynin, a known inhibitor of this enzyme, also yielded nearly identical results in relation to superoxide inhibition[121]. This study suggests that high basal oxidative stress impairs the production and signalling of growth factors during ischemia, implying that high levels of ROS inhibit CCG. But by inhibiting ROS completely, the redox state of the tissue gets overly reductive, again impairing CCG. It seems there is a certain redox state, a so-called "redox window", that not only is permissive for vascular growth, but in which vascular growth can be magnified[85].

2. Hypothesis

The underlying hypothesis of this work was that G-CSF could stimulate coronary collateral growth (CCG) in a rat model of repetitive episodic ischemia (RI). Because redox signalling is critical for CCG and neutrophils are a rich source of NADPH oxidase and reactive oxygen species (ROS), it was further hypothesized that G-CSF-stimulated CCG was determined by the production of ROS.

3. Methods

3.1 Animal preparation for rat model of collateral growth

Male Sprague-Dawley rats (3–4 mo old, 300–350 g) were used for chronic (5 days) implantation of a pneumatic occluder over the left anterior descending coronary artery (LAD; as described by Toyota *et al.*[96]) to produce repetitive ischemia (RI). Briefly, for surgery, rats were premedicated (ketamine 50 mg/mL plus acepromazine 2.5 mg/mL plus torbuterol 2.0 mg/mL, 0.2 mL/100 g body weight, i.p.) and intubated. Oral intubation (I6-G polyethylene tubing) was done under direct observation of the vocal cords with an otoscope. General anesthesia was introduced and maintained by sevoflurane inhalation (1.0% to 2.0%, with 100% oxygen). Body temperature was controlled at 37°C by an electric heating table. Surgery was performed using aseptic technique. The animal was initially placed on its dorsal side, and after a neck incision, the right carotid artery was isolated, and a PE-50 catheter filled with heparin (10 U/mL)-saline was inserted. This tubing was used for monitoring of systemic hemodynamics, sampling arterial blood, and maintaining the blood volume. Blood pH, PaO_2, $PaCO_2$, and systemic hemodynamics were maintained within physiological ranges throughout the surgery. The animal was repositioned on its right side, and the heart was exposed by left thoracotomy. A mini-pneumatic snare occluder (see the Mini-Pneumatic Snare Occluder section for details) was implanted around the mid to proximal LAD. Confirmation that the occluder was functional, i.e., producing myocardial ischemia, was determined initially by observation of blanching and hypokinesis of the left ventricle (LV) during inflation. Rats were randomly divided into 3 groups based on the type of measurement: coronary blood flow (CBF) (neutron activated microspheres), oxidative stress analysis (Dihydroethidium, DHE) or vascular imaging (micro-CT). CBF was measured during coronary occlusion to determine flows to the normal and collateral-dependent zones (see the Microsphere measurements of myocardial and collateral-dependent blood flow and the Coronary Microvascular imaging with Cryomicrotome sections). After instrumentation and measurements, the chest was closed under positive end-expiratory pressure, and the thoracic cavity was evacuated of air. The occluder was tunnelled subcutaneously and exteriorized between the scapulae. This catheter was protected by a stainless steel spring coil connected to a ring that was secured subcutaneously between the scapulae. After the surgery, analgesic

(buprenorphine 0.05 mg/kg s.c.) and antibiotic (enrofloxacin 10 mg/kg s.c.) compounds were administered. Rats were observed in a recovery cage for 2 hours and then transferred to the animal care facility. For 3 days after the surgery, buprenorphine (0.5 mg/kg BID mixed in strawberry Jello) was taken orally for pain relief. On the fourth day after the surgery, the ischemic protocol was started (see the Experimental Protocol section). After 5 days of the experimental protocol, the rats were anesthetized and the chest was opened by mid thoracotomy. In CBF measurement or DHE analysis groups, the hearts were excised at the end of procedures, and the tissue was prepared for analyses.

3.2 Mini-Pneumatic Snare Occluder for Rat Heart

A mini-pneumatic snare occluder consisting of a mini-balloon, sheath tubing, suture, and catheter (**Fig. 11**) was placed on the LAD of the rat heart. The balloon (7 mm long) is made of soft latex membrane and is sufficiently pliable to give negligible physical force on the coronary vessels during balloon deflation. The balloon is mounted within an umbrella sheath (3.2 or 4.8 mm in diameter, 12 mm in length; protects the balloon from fibrous infiltration). Prolene (5– 0) is passed around the LAD and attached to the sheath, securing the occluder to the heart, so that myocardial ischemia is produced by balloon inflation. Inflation volume is small (0.2 to 0.25 mL air), but occlusion occurs by 2 physical actions: “crimping” the LAD toward upward/outside and compressing the LAD by the inflated balloon/sheath. The balloon is connected to a catheter (PE-50) that is exteriorized. Balloon inflation and deflation are controlled from outside the rat cage.

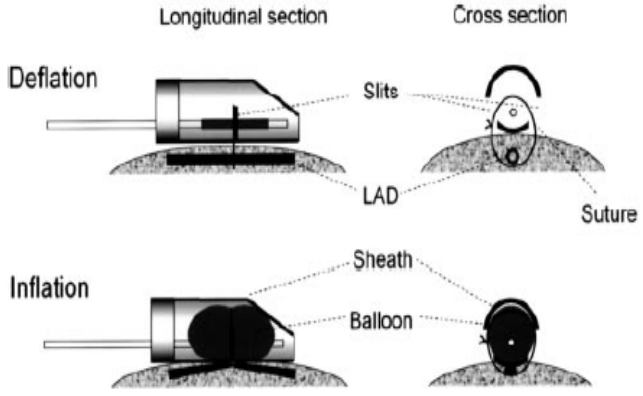

Fig. 11 - Schematic diagram of the mini-pneumatic snare and its actions. Top: Cross-sectional and longitudinal views when the balloon is deflated. Bottom: Views during inflation. The artery is patent when the balloon is deflated, but during inflation, a snare situated underneath the artery is pulled “upward” during inflation, producing the coronary occlusion[94].

3.3 Experimental Protocol

The RI protocol for rat consisted of eight 40sec occlusions, one every 20min over 2h 20min followed by a period of "rest" for 5h and 40min. This 8h cycle was repeated three times per day over a period of 5 days. Blood was collected from the animals at the beginning and end of surgical procedures, for hematological profile of groups. The LAD was occluded automatically by remote inflation or deflation through the catheter. G-CSF at a dose of 100 μg/kg/day (s.c.) was given for 5 days in the specified groups. Measurements were undertaken in the following groups (n=6/group): a sham-operated group that was instrumented but not subjected to RI; a control group/RI; G-CSF, an instrumented group but not subjected to RI; G-CSF+RI; Vehicle+RI (Vehicle=diluting solution of G-CSF: Sodium acetate 10 mM pH 4.2; Sorbitol 200 mM; 0.004% Tween-80); G-CSF+Apocynin (inhibitor of NADPH oxidases, 0.25mg/mL in drinking water, n=3); G-CSF+RI+Apocynin (n=3).

3.2 Microsphere measurements of myocardial and collateral-dependent blood flow

CBF was measured with neutron activated microspheres (Biopal, 15 μm) before initiation of (after all the instruments had been implanted at the time of the initial surgery) and at the end of the repetitive occlusions (when the rats were anesthetized and the chest was open to mimic the conditions of the first measurement) to measure normal zone flows and flow in the developed collaterals. For the first measurement, neutron activated microspheres labelled with Samarium were mixed with fluorescent (FITC) microspheres (Invitrogen, 10 μm) to identify the collateral-dependent region as described below. For the second measurement, Gold labelled microspheres were used. The microspheres (5×10^5) were injected directly into the LV cavity via the LV apex during LAD occlusion with a 29-gauge insulin syringe over a 10-second period. During the course of the procedures, systemic pressure and heart rate were recorded (386-BIOS, American Megatrends Inc). The heart was excised and fresh LV was sliced along the short axis and observed with a dissecting microscope and fluorescent light source. The collateral-dependent area (ischemic zone, LAD region) was distinguished as the

area without fluorescent microspheres. The control area (non-LAD LV region) was determined by the area of distribution of the fluorescent microspheres. The normal and collateral-dependent zones were divided with a blade, and for each the total weight was measured. Collateral flow was calculated as a ratio between activity (dpm/g) of the tissue samples from the LAD-dependent and normal zones.

3.3 Coronary Microvascular imaging with Cryomicrotome

One of each group of rats was prepared for coronary vascular visualization with microcomputed tomography (Micro-CT, *n*=3/group). Rat heart sectioning was performed with the imaging cryomicrotome as described previously[122]. In brief, after sacrifice of the animals, perfusion of the rat heart was continued until the efflux was clear of blood. Subsequently the perfusate was replaced by Batson #17 Solution which was made fluorescent by dissolution of 39μg/mL Potomac yellow, infused at 85 mmHg. Next, the heart was embedded in 5cm diameter cylindrical container filled with 5% carboxymethylcellulose solution containing 5% Indian ink, and frozen at -20°C for at least 24 hours. The specimen was placed in the cryomicrotome which was maintained at -20ºC, after which serial slices were made of 17μ thickness and the remaining bulk tissue was imaged with a 2000x2000 pixel CCD Camera (Kodak Megaplus 4.2i CCD 8 bits grayscale camera), which was custom fitted with a Nikon Lens (Nikon Zoom Lens 70-180mm). The magnification and slice thickness were set so that each tissue voxel represented 17 cubic micrometers. Fluorescent images were acquired with use of 440/20nm excitation and 505/30nm emission band pass filters (Chroma Technology Corp., Rockingham, VT, USA) in combination with a 250W Xenon lamp. Three dimensional image representations were acquired by using Amira 3.1 Software.

3.4 Measurement of oxidative stress

Superoxide production was evaluated by using dihydroethidium (DHE, Inovitrogen) *in vitro* and *in vivo*. Dihydroethidium (also called hydroethidium or hydroethidine) is the chemically reduced form of the commonly used DNA intercalating dye ethidium bromide. Intracellular oxidant stress can be monitored by measuring

changes in fluorescence resulting from intracellular probe oxidation. DHE enters the cell and is oxidized by ROS, particularly superoxide, to yield fluorescent ethidium. Ethidium binds to DNA (Eth-DNA), further amplifying its fluorescence. Eth-DNA fluorescence is generally stable but can be decreased by hydroxyl radical attack. Thus increases in DHE oxidation to Eth-DNA (i.e., increases in Eth-DNA fluorescence) are suggestive of superoxide generation. DHE itself shows a blue fluorescence (absorption/emission: 355/420nm) in cell cytoplasm until oxidization to form ethidium which becomes red fluorescent (absorption/emission: 518/605 nm) upon DNA intercalation. Only once it is internalized and dehydrogenated (oxidized) to ethidium, it can intercalate into DNA. DHE is a neutral probe and is able to penetrate the cell membrane of living cells, staining their cytoplasm blue as well as the chromatin/nucleus red. DHE typically exhibits a uniform labelling of cells within 15 minutes.

For the *in vitro* studies in freshly isolated cardiomyocytes (Cardiomyocyte Isolation for details), G-CSF was administered for 10 min (total treatment time 30 min), and DHE was added during the last 20 min of treatment with G-CSF. Cells were then immediately observed under a fluorescent microscope. For *in vivo* studies, DHE was injected into the LV (60 μg/kg, *n*=3/group) for 20 min before two consecutive periods of ischemia-reperfusion (40s occlusion followed by 20min reperfusion and another 40s occlusion and 20min reperfusion). Animals were then sacrificed. The heart was removed, frozen in optimum cutting temperature compound on dry ice, and stored at -80°C until sectioning. Sections (5 μm) were made in a cryomicrotome and were mounted on glass slides. DHE fluorescence was detected with excitation/emission at 518/605 nm. All images were analyzed at the same microscope settings, and fluorescence intensity was obtained by Metamorph Software on three hearts (10 sections per heart).

3.5 Immunohistochemical analysis

Cryofrozen hearts were sectioned at 5 μm, and mounted on slides. Heart sections were fixated with pre-cooled acetone (10 min) at room temperature. Slides were afterwards rinsed with TBS (4× 5 min), to reduce surface tension and diminish background. Sections were then incubated with blocking solution (10% normal serum

from species of secondary antibody, goat, in Tris 3%-PBS buffer) for 60 min. Blocking solution was aspired and a pre-diluted polyclonal anti-myeloperoxidase (rabbit, Abcam) antibody was added for 1h at room temperature. After washing with PBS (6× 5 min), a FITC secondary antibody was added (goat, dilution 1/500) and slides incubated in the dark for 45 min. Another washing step followed in the dark (PBS, 6× 5 min), previous to mounting and cover slipping of sections with anti fading agent (VectaShield hard-set). The slides were observed and analyzed using a fluorescence microscope.

3.6 Cardiomyocyte isolation

Adult ventricular myocytes were isolated from male Sprague-Dawley rats (250-300 g). Rats were heparinized (300 U i.p.) and anesthetized with ketamine (90 mg/kg) and xylazine (10 mg/kg). Hearts were removed and retrogradely perfused for 15 min in Krebs-Henseleit buffer (KHB, in mM: 118 NaCl, 4.7 KCl, 1.2 $MgSO_4$, 1.2 KH_2PO_4, 25 $NaHCO_3$, 11 glucose) containing 5 mM pyruvate and Liberase Blendzyme (0.1 mg/ml). Calcium was gradually added during the final 10 min of digestion to a concentration of 1.0 mM. Ventricles were minced and placed in KHB containing Liberase for 10 min in a shaking water bath at 37 ºC and dispersed by trituration. The digested tissue was filtered through a 210 μm nylon mesh and the filtrate was centrifuged at 50g for 5 min. Pelleted cells were resuspended in DMEM and plated at a density of 50,000 rod shaped cells per well on 24-well plates precoated with laminin (1μg/cm^2). After 2h, wells were washed with DMEM to remove unattached cells and debris.

3.7 Inhibitors and chelators of ROS Generation

The following metabolic inhibitors and chelators were used to inhibit ROS generation in isolated cardiomyocytes subjected to G-CSF treatment: 1) apocynin (300 μM): an inhibitor of NADPH oxidases to determine if NADPH functions as an electron donor for oxidant generation in cardiomyocytes stimulated with G-CSF; 2) MnTMPyP [Mn(III)Tetrakis(1-methyl-4-pyridyl)porphyrin pentachloride] (100 μM): a cell-permeable superoxide dismutase mimetic which catalyzes the dismutation of superoxide. Treatments were conducted in n=4, as follows: Control (no treatment), G-

CSF (0,05μg/mL), G-CSF (0,1μg/mL), G-CSF (0,3μg/mL), G-CSF(0,3μg/mL)+Apocynin, G-CSF(0,3μg/mL)+MnTMPyP. DHE (5μM) was added in the last 20 min of treatment and cells were observed under a fluorescent microscope.

3.8 Human Coronary Artery Endothelial Cell culture

Human Coronary Artery Endothelial Cells (HCAEC) and optimized media for their growth were purchased from Clonetics and were cultured at low passages (passages 3–8) in Clonetics EGM-2 Bullet Kit medium (Lonza) that contains 25% fetal bovine serum (FBS), 0.2% hydrocortisone, 2% human fibroblast growth factor-b (FGF-B), 0.5% insulin-like growth factor-I (IGF-I), 0.5% ascorbic acid, 0.5% human epidermal growth factor (EGF), and 0.5% Gentamicin/Anphotercin (GA-1000).

3.9 Endothelial tube formation promoted by G-CSF cardiomyocyte stimulation media

Adult ventricular myocytes were isolated and plated as described on point 3.6 above. Cardiac myocytes were stimulated with G-CSF (0.3μg/mL) for 2 and 24 hours. This stimulation media was isolated and used to evaluate HCAEC tube formation. This essay system allows the assessment of a number of cellular events such as attachment, migration, invasion and differentiation in the angiogenesis process. Matrigel (BD Biosciences) was allowed to polymerize for 30 minutes at 37ºC and 5% CO_2 environment on 24-well plates. HCAECs suspensions were prepared by trypsinizing the cell monolayers and resuspending the cells in culture medium with 10% serum at $4x10^5$ cells/mL. HCAECs were than seeded on Matrigel in EGM-2 Bullet Kit medium at a density of 30 000 cells/well. Cells were allowed to attach for 24 h before the addition of 50 ng/ml Regular Media (negative control), VEGF (positive control), 2h G-CSF cardiomyocyte stimulation media, 24h G-CSF cardiomyocyte stimulation media, 2h media + Apocynin (300 μM), 24h media + Apocynin. The extent of tube formation was quantified after 24h by superimposing a grid ($25mm^2$/cube) on microscopic images, and the number of squares containing tubes were counted and

averaged from five randomly selected fields for each well to obtain the percentage of total field that contained tubes. Treatments were conducted in n=4.

3.9 Data analysis

ANOVA followed by *t*-tests was used for statistical analysis. A probability value of $P<0.05$ was used to determine statistical significance.

4. Results

4.1 Specificity of G-CSF

Through collection of blood samples in the beginning and in the end of the surgical procedures it was possible to evaluate the hematological profile of each group (**Fig. 12**) as well as the specificity of the treatment. G-CSF (100 μg/Kg/day) proved to be a specific promoter of neutrophil counts in the peripheral blood because only neutrophil granulocytes but not monocytic cells were increased by the treatment with G-CSF. Another fact worth mentioning is the increase in neutrophil numbers in the Vehicle+RI group in comparison with the numbers of neutrophils before the surgery and after the complete inhibition of neutrophil production by apocynin.

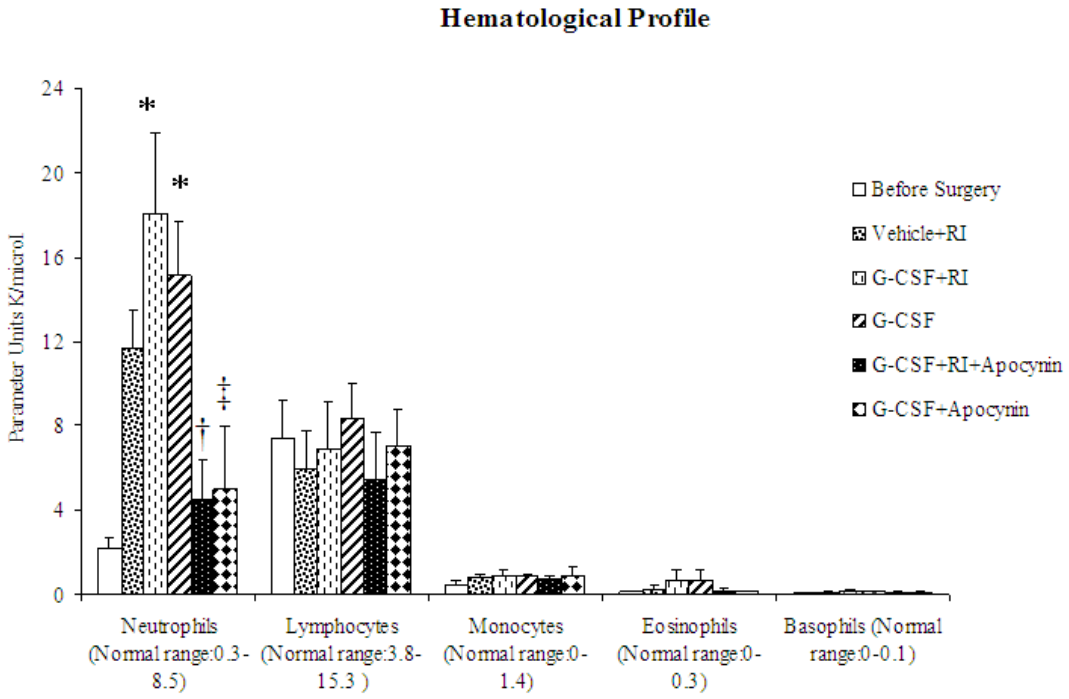

Fig. 12 – Hematological profile of the animal groups. Normal range of blood cells in peripheral blood is expressed in 1000/μL. Neutrophil numbers before surgery (2.13 ± 0.59); after RI+Vehicle (12.17 ± 2.36); RI+G-CSF (18.05 ± 3.84); G-CSF alone (15.12 ± 2.61). *n*=6/group, means±SE. * *vs*. vehicle, † *vs*. G-CSF+RI, ‡ *vs*. G-CSF NoRI, $P<0.01$.

4

4.2 G-CSF induces Coronary Collateral Growth (CCG)

Evaluation of collateral growth was performed after completion of the protocol by a simple functional test: total coronary occlusion. The rationale for this procedure was that if collaterals were developed, then occlusion would not induce functional disturbances. Alternatively, if collaterals were not mature, then occlusion would cause hemodynamic disturbances. After the second measurement of coronary blood flow, the coronary occlusion was maintained, systemic hemodynamics were measured and also the number of arrhythmias. In animals without collaterals, coronary occlusion caused deterioration of systemic hemodynamics and arrhythmias, including premature ventricular contractions, ventricular tachycardia, and ventricular fibrillation; in animals with well developed collaterals, no such adverse effects were noted.

In order to delineate the area of the myocardium dependent on LAD blood flow, as described in the methods section, fluorescent microspheres were injected in the beginning of the procedures while the LAD was occluded. After the completion of treatments, the heart was removed, and the left ventricle (LV) was sliced along the short axis and observed with a dissecting microscope under fluorescent light. The collateral-dependent area (LAD region, ischemic zone) was distinguished as the area without fluorescent microspheres. The control area (non-LAD LV region, normal zone) was determined by the area of distribution of the fluorescent microspheres (**Fig. 13**).

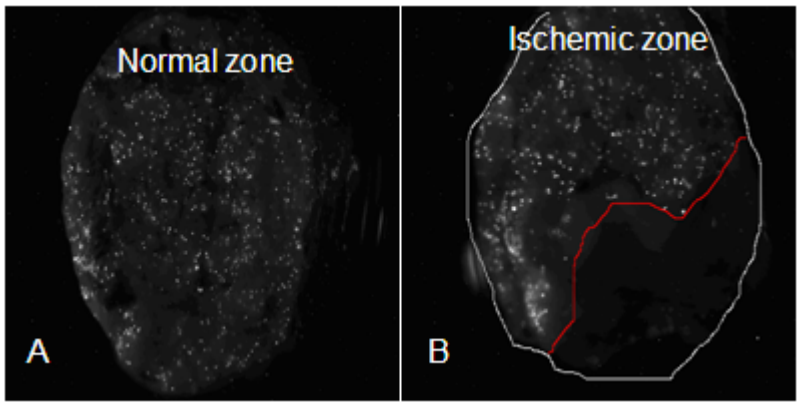

Fig. 13 – Isolation of normal and ischemic zones for collateral blood flow measurements. A=normal zone; B=ischemic zone.

The normal and collateral-dependent zones were divided with a blade, and each total weight was measured. Collateral flow was calculated as a ratio between radioactive decay (dpm/g = disintegration per min/gram) of the tissue samples from the LAD-dependent and normal zones. Increase in CCG is expressed as the variation (Δ) of CBF before (1st day) and after treatments (5th day). Following RI, G-CSF increased CCG (0.47 ± 0.15) *versus* vehicle (0.14 ± 0.06, P<0.01). Surprisingly, G-CSF treatment without RI increased CCG (0.57 ± 0.18, P<0.01 *vs*. vehicle) equal to G-CSF + RI (**Fig. 14**).

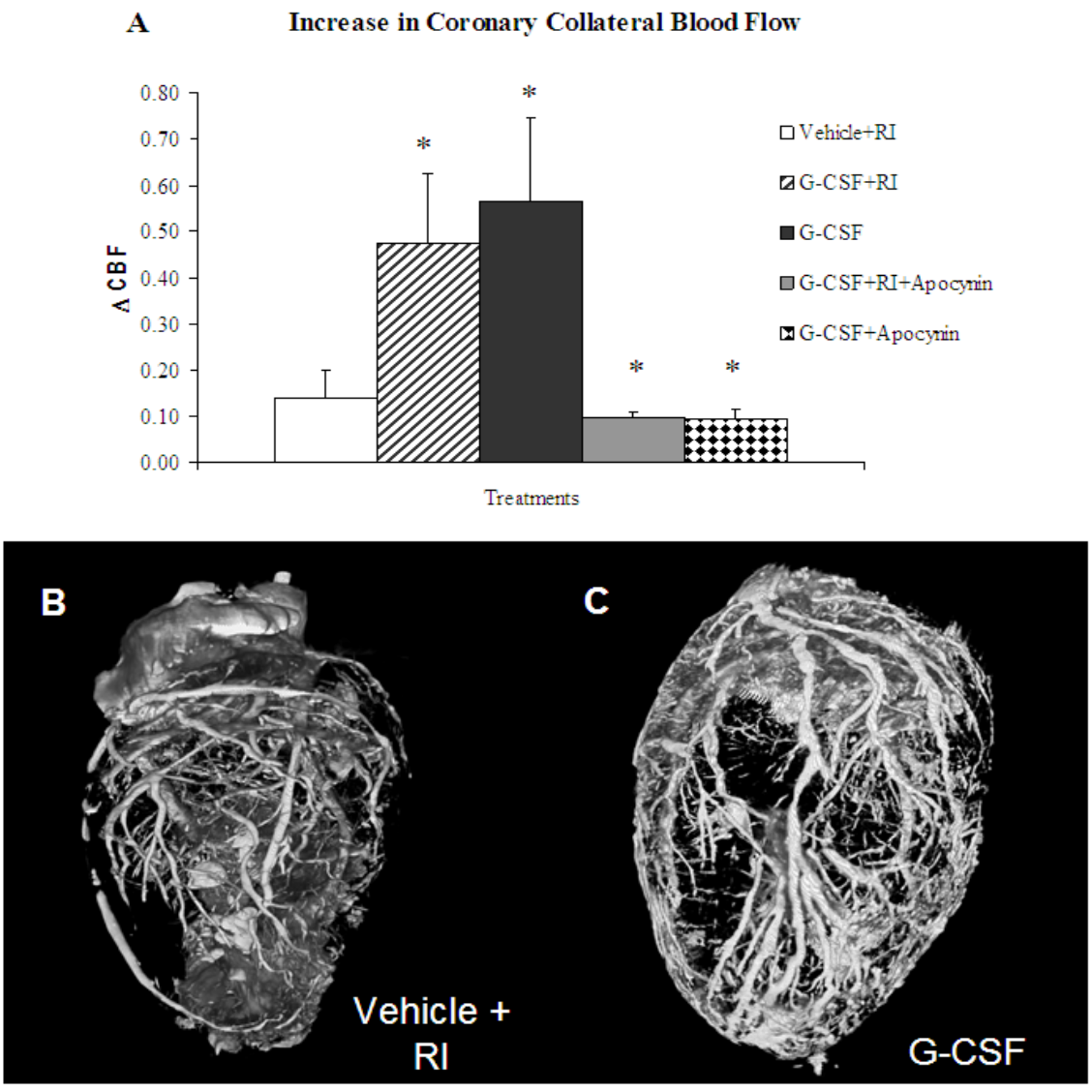

Fig. 14 – *A:* Coronary Collateral Blood Flow (CBF) expressed as variation (delta) between first and fifth day of treatment in samples from LAD-dependent and normal zones. Vehicle+RI (0.14±0.06); G-CSF+RI (0.47±0.15); G-CSF (0.57±0.18); G-CSF+RI+Apocynin (0.09±0.01); G-CSF+Apocynin (0.09±0.02). *n*=6/group, means±SE. Micro-CT images of Vehicle+RI (**B**), G-CSF treated hearts (**C**). **vs*. vehicle+RI *P*<0.05.

4.3 G-CSF Induces ROS Production

Dihydroethidium (DHE) was injected into the LV (60 μg/kg, *n*=3/group) for 20 min before two consecutive periods of ischemia-reperfusion, that is, 40s occlusion followed by 20 min reperfusion and another 40s occlusion and 20 min reperfusion. This was intended to determine the levels of superoxide generation in the myocardium. Animals were then sacrificed, and the hearts were removed, frozen and sectioned. DHE fluorescence was detected with microscope visualization, excitation/emission at 518/605 nm, and fluorescence intensity was obtained by Metamorph Software on three hearts per group (10 sections per heart). DHE fluorescence intensity was found to be double in the group of animals treated with G-CSF together with RI stimulation (81.0 ± 2.6) *versus* vehicle+RI (40.6 ± 3.8, $P<0.01$). Unexpectedly, even higher levels of DHE fluorescence were found in the group of animals treated with G-CSF without RI induction (107.9 ± 9.6, $P<0.01$; see **Fig. 15,** next page).

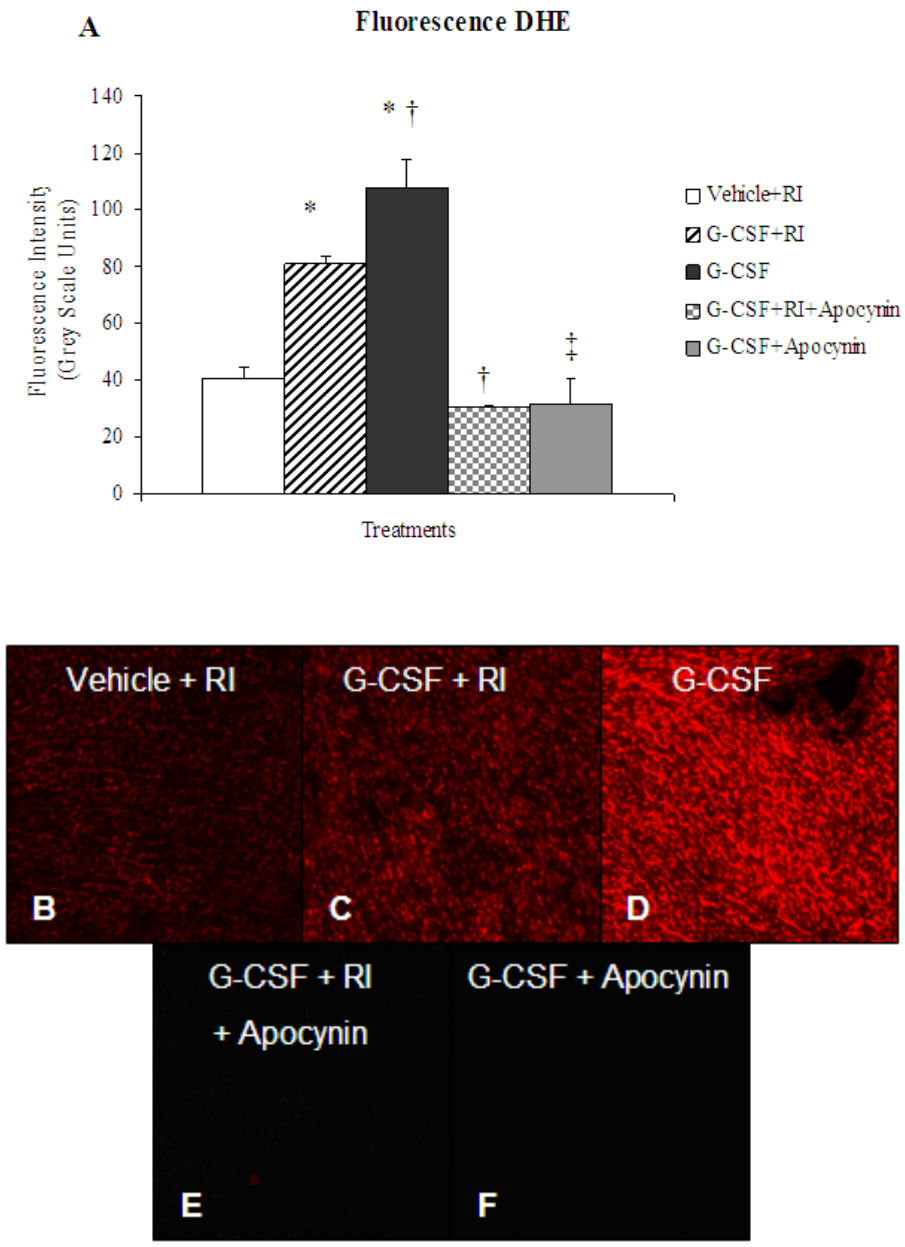

Fig. 15 – *A:* Fluorescence intensity of Dihydroethidium (DHE) injected into LV (60 µg/kg) before two consecutive periods of repetitive ischemia. Vehicle+RI (40.6±3.8); G-CSF+RI (81.0±2.6); G-CSF (107.9±9.6); G-CSF+RI+Apocynin (30.6±0.6); G-CSF+Apocynin (31.6±9.0). *n*=3/group in 10 sections/heart, means±SE. **vs.* vehicle, †*vs.* G-CSF+RI, ‡*vs.* G-CSF, *P*<0.01. ***B-F:*** Photographs of DHE fluorescence (Magnification 10×).

4.4 Myeloperoxidase does not co-localize with ROS

To be able to determine which cell type was responsible for the increased DHE signal, myeloperoxidase (MPO, a neutrophil marker) immunostaining was undertaken in heart sections of the treated groups. It was interesting to find that the DHE signal did not co-localize with MPO, a peroxidase enzyme present in neutrophil granulocytes. The immunostaining with myeloperoxidase led to the conclusion that the signal for the ROS creation (DHE fluorescence) appeared mostly in cardiac myocytes and not in granulocytes (**Fig. 15-16**).

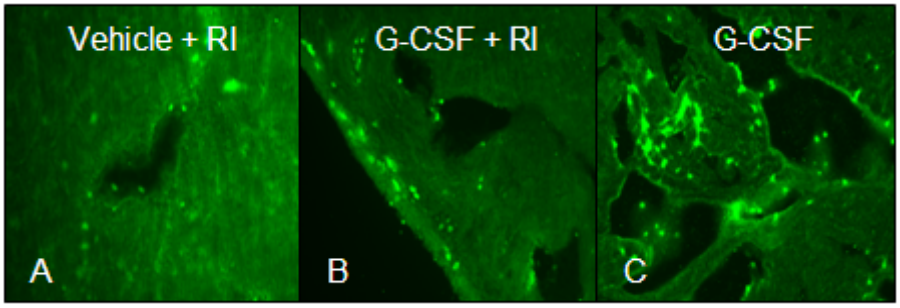

Fig. 16 – Immunostaining of Myeloperoxidase (MPO). Green dots represent granulocytes in the myocardium. Original magnification is 20× for A, 10× B and C. Data shown is representative of 3 separate experiments.

4.5 G-CSF directly stimulates cardiomyocytes to produce ROS

To clearly determine if G-CSF directly stimulates ROS production in cardiac myocytes, it was necessary to study isolated cardiac myocytes. The administration of different concentrations of G-CSF (0.05, 0.1, 0.3 μg/mL) to isolated cardiomyocyte culture confirmed a substantial increase in ROS production in comparison with untreated controls. The inhibition of NADPH oxidase by apocynin (300μM) or the administration of the cell-permeable superoxide dismutase/catalase mimetic, MnTMPyP (100μM) completely abolished the DHE signal (**Fig. 17**), cancelling ROS production in isolated cardiomyocyte cultures.

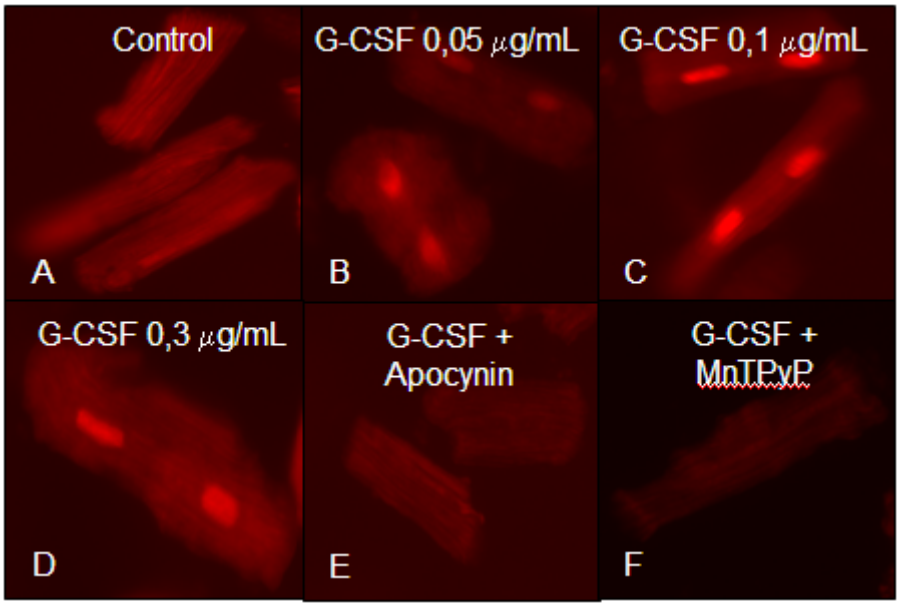

Fig. 17 – Production of ROS by isolated cardiac myocytes revealed by DHE fluorescence (5μM). **A:** Control, not subjected to treatment. **B-D:** G-CSF different concentrations (0.05, 0.1, 0.3μg/mL). **E:** G-CSF (0.3μg/mL) + apocynin (300μM, inhibitior NADPH oxidase) abolished DHE signal. **F:** G-CSF (0.3μg/mL) + MnTMPyP (100μM, superoxide dismutase mimetic) revealed that the DHE fluorescence was due to superoxide production.

4.6 Apocynin inhibits coronary collateral growth

To be able to understand if the direct stimulation of ROS production in cardiac myocytes by G-CSF was critical for collateral growth, additional studies were carried out with groups of animals that received apocynin in drinking water and were subjected to G-CSF treatment with and without RI. Apocynin prevented coronary collateral growth in all groups, whether with or without repetitive occlusions: G-CSF with RI, 0.47± 0.15 *vs.* Apocynin + G-CSF + RI, 0.09 ± 0.01 ($P<0.01$); G-CSF with no RI stimulation, 0.57 ± 0.18 *vs.* Apocynin + G-CSF + No RI, 0.09 ± 0.02 ($P<0.01$, **Fig. 14**). Moreover, DHE fluorescence intensity was completely abolished by apocynin in both groups, G-CSF + RI (81.0 ± 2.6 *vs.* 30.6 ± 0.6, $P<0.01$) and G-CSF + No RI (107.9 ± 9.6 *vs.* 31.6 ± 9.0, $P<0.01$; **Fig. 14-15**).

4.7 Endothelial tube formation promoted by G-CSF cardiomyocyte stimulation media

In order to clarify whether the cardiomyocytes that were being stimulated by G-CSF were producing a medium that was rich in angiogenic factors which could promote vascular growth, the next experiments carried out were tube formation assays with human coronary artery endothelial cells (HCAEC). Isolated cardiomyocytes were stimulated with G-CSF for two different periods of time (2 and 24h). These media were than isolated and used to evaluate tube formation of HCAEC cultures in matrigel. As seen in **Fig. 18** (next page), 2h G-CSF-cardiomyocyte-stimulating-medium already promoted tube formation in similar values as VEGF positive control (5.6 ± 1.9 *vs.* 5.5 ± 1.2, respectively). Furthermore, 24h of G-CSF stimulation time further increased the percentage of area covered by new tubes (9.7 ± 0.5). After using apocynin as a NADPH oxidase inhibitor, there was a clear abolishment of tube formation in both periods of time in comparison with the respective groups, 2h (1.0 ± 0.1) and 24h (0.9 ± 0.1).

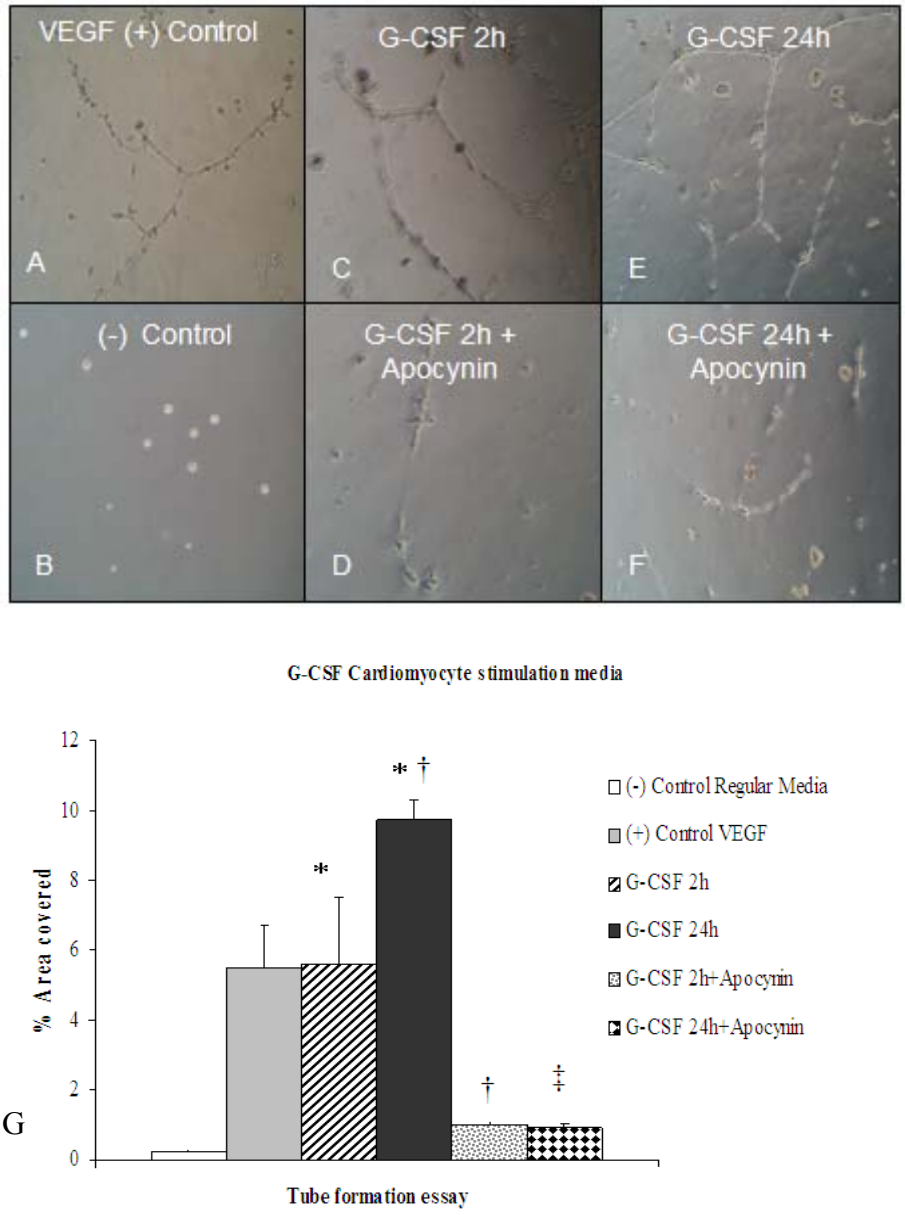

Fig. 18 – Human coronary artery endothelial cell (HCAEC) tube formation in Matrigel.

***A-F*:** Images of tube formation after addition of G-CSF cardiomyocyte stimulation medium and apocynin (300μM/L), as indicated.

G: percentage of area covered with tubes (n=4/group, means±SE).

**vs*. VEGF, †*vs*. G-CSF 2h, ‡*vs*. G-CSF 24h, P <0.01.

5. Discussion

By the analysis of the results obtained, the major observation of this study was that G-CSF *per se* can stimulate coronary collateral growth. According to the results, G-CSF with or without repetitive ischemia stimulation, is able to promote the necessary remodelling in the myocardium to promote coronary collateral growth. This was a surprising occurrence, because in the beginning of the study it was predicted that G-CSF in the absence of ischemia would not initiate coronary collateral growth. It is well known that after an initial ischemic event, an array of cytokines, complement components and cell contents are released, inducing the recruitment of neutrophil granulocytes to the ischemic site, which, as several studies have shown, play an important role in the ischemic insult of the myocardium[56,123]. A detailed observation of the results provided a possible resolution to the question how G-CSF could initiate collateral growth in the absence of ischemia. Particularly, it was found that administration of G-CSF increased ROS production directly in cardiac myocytes. This event could be a mimesis of the well known occurrence of enhanced ROS production during myocardial ischemia-reperfusion, suggesting that G-CSF to some extent may act as a substitute or surrogate for certain aspects of myocardial ischemia. Furthermore, it was observed in isolated cardiac myocytes, that G-CSF-induced ROS production is associated with the release of angiogenic factors into the culture medium which consequently promote tube formation by coronary artery endothelial cells, again mimicking the actions of the ischemic heart[124].

The observations and conclusions revealed by this study are supported by some cogent work in the literature. It has been reported that G-CSF has direct and acute protective effects on the myocardium against ischemia-reperfusion injury. Ueda *et al.*[70] have demonstrated that G-CSF directly inhibits myocardial ischemia-reperfusion injury and has acute non-genomic cardioprotective effects through an Akt-endothelial NOS pathway. It has also been shown that G-CSF acts directly on cardiomyocytes and induces survival signals in post-MI hearts. Harada *et al.*[38] have shown that G-CSF can promote the survival of cardiac myocytes and prevent left ventricular remodelling after myocardial infarction through a functional communication between cardiomyocytes and non-cardiomyocytes.

The results presented in this thesis show for the first time that G-CSF can promote coronary collateral growth with or without ischemic stimulus. Previously,

Toyota *et al.*[96] have proven that augmentation in coronary collateral flow reveals an increase in the calibre of the collateral vessels, therefore the reason for the relative blood flow increase after G-CSF treatment (in comparison with RI alone) is through the specific growth of these vessels.

G-CSF in the absence of repetitive ischemia also enhanced the levels of coronary collateral growth, which was rather intriguing and it could suggest that the cytokine mimics certain effects of ischemia itself. The results provided by this study and from others bear upon this suggestion. With this work, it was found that treatment of isolated myocytes with G-CSF stimulated the production of angiogenic growth factors in a ROS-dependent manner. It is well-known that ischemia-reperfusion produces a burst of ROS that stimulates many adaptations of the ischemic heart, including coronary collateral growth[125-127]. Rocic *et al.*[125] have demonstrated the requirement of ROS for coronary collateral development through a p38MAP kinase activation mechanism. Liu *et al.*[115] have concluded that redox signalling prior to an ischemic period is an essential step to trigger the protected state that is promoted by ischemic preconditioning and that ROS creation occurs in a early step of this signalling cascade. Furthermore, G-CSF was found to promote neovascularization by releasing VEGF from neutrophils and bone marrow derived cells of hematopoietic lineage[64, 128]. Ohki *et al.*[64] clearly have shown that G-CSF modulates angiogenesis in ischemic tissue by increasing neutrophils that are VEGF receptor-1 positive ($VEGFR1^+$) and the consequent release of VEGF by these cells. Powell and colleagues[128] have demonstrated that patients with coronary artery disease that were treated with G-CSF had higher levels of endothelial progenitor cells in the circulation, proposing that these cells would be useful for initiation of vascular growth and cardiomyocyte repair in these patients. Toyota *et al.* [96] also have revealed that expression of VEGF is critical to the growth of coronary collaterals. Under G-CSF stimulation, it seems that the production of VEGF and ROS are also essential for the remodelling that occurs in the myocardium. Zhu and colleagues[54] have shown that G-CSF induces ROS production in peripheral blood cells and that G-CSF–induced ROS production is dependent on NADPH oxidase. It has also been demonstrated that coronary collateral development in this specific rat model of RI is critically dependent on an optimal concentration of ROS generated in the myocardium[125].

Although it was initially thought that G-CSF would trigger neutrophil immigration to the myocardium under a RI stimulus and that these neutrophils would be

responsible for ROS production, what was observed was that G-CSF directly stimulated cardiomyocytes to generate ROS. The results obtained by studying isolated cardiomyocytes clearly demonstrate that G-CSF is acting directly on cardiomyocytes to produce ROS, and that this ROS generation is critical for the production of angiogenic growth factors in response to G-CSF stimulation of the myocytes. The results of this study are also consistent with the conclusion that G-CSF mediated induction of cardiomyocyte-ROS is dependent on a NADPH oxidase mechanism, since apocynin, an inhibitor of NADPH oxidase assembly, cancelled the effect promoted by G-CSF both *in vivo* and *in vitro*. Apocynin inhibits the release of superoxide anion by NADPH oxidase by blocking the migration of the cytosolic component p47phox to the membrane, a critical step to initiate the assembly of the functional NADPH oxidase complex[129-131]. The results obtained in this study encourage to think that the mechanism by which G-CSF is acting in cardiac myocytes is similar to the one revealed recently by Zhu *et al.*[54] in neutrophils. It was shown by this group that in neutrophils, G-CSF induces ROS production via NADPH oxidase through phosphorylation of p47phox by Akt, allowing the recruitment of this sub-unit to the membrane and the consequent functionality of NADPH oxidase. Further work is needed to verify this mechanism in cardiomyocytes, although there is some evidence in the literature that this is the accurate way. Heymes *at al*.[132] were the first group to report the presence of NADPH oxidase in human myocardium. Although the overall level of the enzyme was unaltered in failing compared with non-failing hearts, there was an increase in the translocation of the regulatory sub-unit, p47phox, to the membranes of the myocytes in the failing hearts. More recently, Borchi *et al*.[133] have shown that in cardiac muscle cells exposed to stimulated ischemia-reperfusion there was an increase in Nox2 expression and p47phox translocation to the membrane, providing more evidence that NADPH oxidase is a key enzyme involved in this cardiac mechanism.

The data presented in this work induce the hypothesis that G-CSF may be acting as a surrogate of myocardial ischemia, inducing *per se* positive adaptations in the myocardium by the same means employed by ischemic-preconditioning, i.e., ROS production in cardiomyocytes and coronary collateral growth.

6. Conclusions

In conclusion, this study demonstrates the induction of coronary collateral growth by G-CSF. The data presented here provide evidence that this mechanism is mediated by ROS that are directly produced in cardiac myocytes. Another effect of G-CSF on cardiomyocytes is the generation of angiogenic factors that seem to be essential for the vascular remodelling that takes place. The results obtained give rise to the hypothesis that G-CSF may be acting as a surrogate for myocardial ischemia in the stimulation of coronary collateral growth.

7. Recommendations

As always in science, there are many questions still unanswered regarding G-CSF's actions in the myocardium. First of all, although it is suggested by this work and supported by strong evidence from the literature that G-CSF is inducing ROS production via NADPH oxidase through phosphorylation of p47phox by Akt, allowing the recruitment of this sub-unit to the membrane and the consequent functionality of NADPH oxidase, further work is needed to verify the existence of this mechanism in cardiomyocytes. A second point that is worth mentioning is the lack of knowledge about which angiogenic factors are being produced by the G-CSF-stimulated cardiac myocytes. Although it is compelling to think that VEGF is one of the major players, VEGF alone does not explain the massive increase in the ability of endothelial cells to rearrange themselves in angiogenic tubes by the G-CSF cardiomyocyte stimulation medium. Certainly, other factors are being produced and it would be of interest to determine which. Another point that is still left unanswered is the specific role of the neutrophil granulocytes in this setting. Several studies explain the negative effects that neutrophils and myeloperoxidase have in ischemia-reperfusion, atherosclerosis or acute coronary syndrome[56, 134, 135]. But, in this study, the raise of peripheral neutrophil numbers by G-CSF does not seem to exert negative effects in the heart of a young animal, on the contrary. Further studies will be needed to help clarify possible negative outcomes coupled with G-CSF treatment.

G-CSF has been used as an adjunctive therapy in patients with AMI for some years. Clinical trials have been published and G-CSF treatment seems to be a safe therapy. Initial unblinded trials in patients with AMI were encouraging in regard to the results obtained. However, larger double-blind placebo-controlled trials have not been able to demonstrate an improvement of myocardial recovery after G-CSF treatment in the setting of AMI [136-138]. There are many controversies in the interpretation of these clinical trial results: about the importance of direct effects of G-CSF in the myocardium *vs.* indirect effects through bone marrow progenitor cell mobilization; the importance of timing and dosage of G-CSF therapy; the importance of cell types that are being mobilized by G-CSF; about the heterogenous age and clinical history of the patients involved in the clinical trials.

The results obtained with this study give further emphasis on the direct effects that G-CSF has on the myocardium and bear the possibility of utilizing G-CSF not as an

acute treatment of heart failure but as a prophylactic agent in patients with coronary heart disease. Cell-based therapies to improve cardiac function remain promising and further experimental and clinical studies are needed to determine the future role of G-CSF.

8. References

1. Basu S, Dunn A, Ward A. G-CSF: function and modes of action (Review). *Int J Mol Med.* 2002;10:3-10.
2. Bradley TR, Robinson W, Metcalf D. Colony production in vitro by normal polycythaemic and anaemic bone marrow. *Nature.* 1967;214:511.
3. Demetri GD, Griffin JD. Granulocyte colony-stimulating factor and its receptor. *Blood.* 1991;78:2791-2808.
4. Byrne PV, Heit W, Kubanek B. Stimulation of in vitro granulocyte--macrophage colony formation by mouse heart conditioned medium. *Br J Haematol.* 1978;40:197-204.
5. Burgess AW, Metcalf D. Characterization of a serum factor stimulating the differentiation of myelomonocytic leukemic cells. *Int J Cancer.* 1980;26:647-654.
6. Lotem J, Lipton JH, Sachs L. Separation of different molecular forms of macrophage- and granulocyte-inducing proteins for normal and leukemic myeloid cells. *Int J Cancer.* 1980;25:763-771.
7. Metcalf D. Clonal extinction of myelomonocytic leukemic cells by serum from mice injected with endotoxin. *Int J Cancer.* 1980;25:225-233.
8. Nicola NA, Metcalf D, Matsumoto M, Johnson GR. Purification of a factor inducing differentiation in murine myelomonocytic leukemia cells. Identification as granulocyte colony-stimulating factor. *J Biol Chem.* 1983;258:9017-9023.
9. Nicola NA, Begley CG, Metcalf D. Identification of the human analogue of a regulator that induces differentiation in murine leukaemic cells. *Nature.* 1985;314:625-628.

10. Nomura H, Imazeki I, Oheda M, Kubota N, Tamura M, Ono M, Ueyama Y, Asano S. Purification and characterization of human granulocyte colony-stimulating factor (G-CSF). *Embo J.* 1986;5:871-876.

11. Nagata S, Tsuchiya M, Asano S, Kaziro Y, Yamazaki T, Yamamoto O, Hirata Y, Kubota N, Oheda M, Nomura H, Ono M. Molecular cloning and expression of cDNA for human granulocyte colony-stimulating factor. *Nature.* 1986;319:415-418.

12. Souza LM, Boone TC, Gabrilove J, Lai PH, Zsebo KM, Murdock DC, Chazin VR, Bruszewski J, Lu H, Chen KK, et al. Recombinant human granulocyte colony-stimulating factor: effects on normal and leukemic myeloid cells. *Science.* 1986;232:61-65.

13. Nagata S, Tsuchiya M, Asano S, Yamamoto O, Hirata Y, Kubota N, Oheda M, Nomura H, Yamazaki T. The chromosomal gene structure and two mRNAs for human granulocyte colony-stimulating factor. *Embo J.* 1986;5:575-581.

14. Le Beau MM, Lemons RS, Carrino JJ, Pettenati MJ, Souza LM, Diaz MO, Rowley JD. Chromosomal localization of the human G-CSF gene to 17q11 proximal to the breakpoint of the t(15;17) in acute promyelocytic leukemia. *Leukemia.* 1987;1:795-799.

15. Simmers RN, Webber LM, Shannon MF, Garson OM, Wong G, Vadas MA, Sutherland GR. Localization of the G-CSF gene on chromosome 17 proximal to the breakpoint in the t(15;17) in acute promyelocytic leukemia. *Blood.* 1987;70:330-332.

16. Nicola NA. Hemopoietic cell growth factors and their receptors. *Annu Rev Biochem.* 1989;58:45-77.

17. Tsuchiya M, Asano S, Kaziro Y, Nagata S. Isolation and characterization of the cDNA for murine granulocyte colony-stimulating factor. *Proc Natl Acad Sci U S A.* 1986;83:7633-7637.

18. Fukunaga R, Ishizaka-Ikeda E, Seto Y, Nagata S. Expression cloning of a receptor for murine granulocyte colony-stimulating factor. *Cell Res.* 1990;61:341-350.

19. Kishimoto T. The biology of interleukin-6. *Blood.* 1989;74:1-10.

20. Lieschke GJ, Grail D, Hodgson G, Metcalf D, Stanley E, Cheers C, Fowler KJ, Basu S, Zhan YF, Dunn AR. Mice lacking granulocyte colony-stimulating factor have chronic neutropenia, granulocyte and macrophage progenitor cell deficiency, and impaired neutrophil mobilization. *Blood.* 1994;84:1737-1746.

21. Kaushansky K, Lin N, Adamson JW. Interleukin 1 stimulates fibroblasts to synthesize granulocyte-macrophage and granulocyte colony-stimulating factors. Mechanism for the hematopoietic response to inflammation. *J Clin Invest.* 1988;81:92-97.

22. Kaushansky K, Broudy VC, Harlan JM, Adamson JW. Tumor necrosis factor-alpha and tumor necrosis factor-beta (lymphotoxin) stimulate the production of granulocyte-macrophage colony-stimulating factor, macrophage colony-stimulating factor, and IL-1 in vivo. *J Immunol.* 1988;141:3410-3415.

23. Basu S, Hodgson G, Katz M, Dunn AR. Evaluation of role of G-CSF in the production, survival, and release of neutrophils from bone marrow into circulation. *Blood.* 2002;100:854-861.

24. Nagata S, Fukunaga R. Granulocyte colony-stimulating factor and its receptor. *Prog Growth Factor Res.* 1991;3:131-141.

25. Avalos B. Molecular analysis of the granulocyte colony-stimulating factor receptor. *Blood.* 1996;88:761-777.

26. Zsebo KM, Yuschenkoff VN, Schiffer S, Chang D, McCall E, Dinarello CA, Brown MA, Altrock B, Bagby GC, Jr. Vascular endothelial cells and granulopoiesis: interleukin-1 stimulates release of G-CSF and GM-CSF. *Blood.* 1988;71:99-103.

27. Sallerfors B. Endogenous production and peripheral blood levels of granulocyte-macrophage (GM-) and granulocyte (G-) colony-stimulating factors. *Leuk Lymphoma.* 1994;13:235-247.

28. Basu S, Hodgson G, Zhang H-H, Katz M, Quilici C, Dunn AR. "Emergency" granulopoiesis in G-CSF-deficient mice in response to Candida albicans infection. *Blood.* 2000;95:3725-3733.

29. Sampson M, Zhu QS, Corey SJ. Src kinases in G-CSF receptor signaling. *Front Biosci.* 2007;12:1463-1474.

30. Fukunaga R, Seto Y, Mizushima S, Nagata S. Three Different mRNAs Encoding Human Granulocyte Colony-Stimulating Factor Receptor. *Proceedings of the National Academy of Sciences.* 1990;87:8702-8706.

31. Hermans MHA, van de Geijn G-J, Antonissen C, Gits J, van Leeuwen D, Ward AC, Touw IP. Signaling mechanisms coupled to tyrosines in the granulocyte colony-stimulating factor receptor orchestrate G-CSF-induced expansion of myeloid progenitor cells. *Blood.* 2003;101:2584-2590.

32. Rose TM, Bruce AG. Oncostatin M is a member of a cytokine family that includes leukemia-inhibitory factor, granulocyte colony-stimulating factor, and interleukin 6. *Proc Natl Acad Sci U S A.* 1991;88:8641-8645.

33. Calhoun DA, Donnelly WH, Jr., Du Y, Dame JB, Li Y, Christensen RD. Distribution of granulocyte colony-stimulating factor (G-CSF) and G-CSF-receptor mRNA and protein in the human fetus. *Pediatr Res.* 1999;46:333-338.

34. Takano H QY, Hasegawa H, Ueda K, Niitsuma Y, Ohtsuka M, Komuro I. . Effects of G-CSF on left ventricular remodeling and heart failure after acute myocardial infarction. *J Mol Med.* 2006 84:185-193.

35. Bocchietto E, Guglielmetti A, Silvagno F, Taraboletti G, Pescarmona GP, Mantovani A, Bussolino F. Proliferative and migratory responses of murine microvascular endothelial cells to granulocyte-colony-stimulating factor. *J Cell Physiol.* 1993;155:89-95.

36. Fuste B, Mazzara R, Escolar G, Merino A, Ordinas A, Diaz-Ricart M. Granulocyte colony-stimulating factor increases expression of adhesion receptors on endothelial cells through activation of p38 MAPK. *Haematologica.* 2004;89:578-585.

37. Park KW, Kwon YW, Cho HJ, Shin JI, Kim YJ, Lee SE, Youn SW, Lee HC, Kang HJ, Shaul PW, Oh BH, Park YB, Kim HS. G-CSF exerts dual effects on endothelial cells-Opposing actions of direct eNOS induction versus indirect CRP elevation. *J Mol Cell Cardiol.* 2008.

38. Harada M QY, Takano H, Minamino T, Zou Y, Toko H, Ohtsuka M, Matsuura K, Sano M, Nishi J, Iwanaga K, Akazawa H, Kunieda T, Zhu W, Hasegawa H, Kunisada K, Nagai T, Nakaya H, Yamauchi-Takihara K, Komuro I. . G-CSF prevents cardiac remodeling after myocardial infarction by activating the Jak-Stat pathway in cardiomyocytes. *Nat Med.* 2005;11:305-311.

39. Aarts LH, Roovers O, Ward AC, Touw IP. Receptor activation and 2 distinct COOH-terminal motifs control G-CSF receptor distribution and internalization kinetics. *Blood.* 2004;103:571-579.

40. Hermans MH, Ward AC, Antonissen C, Karis A, Lowenberg B, Touw IP. Perturbed granulopoiesis in mice with a targeted mutation in the granulocyte colony-stimulating factor receptor gene associated with severe chronic neutropenia. *Blood.* 1998;92:32-39.

41. Liu F, Poursine-Laurent J, Link DC. The granulocyte colony-stimulating factor receptor is required for the mobilization of murine hematopoietic progenitors into peripheral blood by cyclophosphamide or interleukin-8 but not flt-3 ligand. *Blood.* 1997;90:2522-2528.

42. Parganas E, Wang D, Stravopodis D, Topham DJ, Marine JC, Teglund S, Vanin EF, Bodner S, Colamonici OR, van Deursen JM, Grosveld G, Ihle JN. Jak2 is essential for signaling through a variety of cytokine receptors. *Cell.* 1998;93:385-395.

43. Rodig SJ, Meraz MA, White JM, Lampe PA, Riley JK, Arthur CD, King KL, Sheehan KC, Yin L, Pennica D, Johnson EM, Jr., Schreiber RD. Disruption of the Jak1 gene demonstrates obligatory and nonredundant roles of the Jaks in cytokine-induced biologic responses. *Cell.* 1998;93:373-383.

44. Corey SJ, Dombrosky-Ferlan PM, Zuo S, Krohn E, Donnenberg AD, Zorich P, Romero G, Takata M, Kurosaki T. Requirement of Src kinase Lyn for induction of DNA synthesis by granulocyte colony-stimulating factor. *J Biol Chem.* 1998;273:3230-3235.

45. de Koning JP, Dong F, Smith L, Schelen AM, Barge RM, van der Plas DC, Hoefsloot LH, Lowenberg B, Touw IP. The membrane-distal cytoplasmic region

of human granulocyte colony-stimulating factor receptor is required for STAT3 but not STAT1 homodimer formation. *Blood.* 1996;87:1335-1342.

46. Songyang Z, Shoelson SE, Chaudhuri M, Gish G, Pawson T, Haser WG, King F, Roberts T, Ratnofsky S, Lechleider RJ, et al. SH2 domains recognize specific phosphopeptide sequences. *Cell.* 1993;72:767-778.

47. de Koning JP, Schelen AM, Dong F, van Buitenen C, Burgering BM, Bos JL, Lowenberg B, Touw IP. Specific involvement of tyrosine 764 of human granulocyte colony-stimulating factor receptor in signal transduction mediated by p145/Shc/GRB2 or p90/GRB2 complexes. *Blood.* 1996;87:132-140.

48. Zhu QS, Robinson LJ, Roginskaya V, Corey SJ. G-CSF-induced tyrosine phosphorylation of Gab2 is Lyn kinase dependent and associated with enhanced Akt and differentiative, not proliferative, responses. *Blood.* 2004;103:3305-3312.

49. Rausch O, Marshall CJ. Tyrosine 763 of the murine granulocyte colony-stimulating factor receptor mediates Ras-dependent activation of the JNK/SAPK mitogen-activated protein kinase pathway. *Mol Cell Biol.* 1997;17:1170-1179.

50. Hunter MG, Jacob A, O'Donnell L C, Agler A, Druhan LJ, Coggeshall KM, Avalos BR. Loss of SHIP and CIS recruitment to the granulocyte colony-stimulating factor receptor contribute to hyperproliferative responses in severe congenital neutropenia/acute myelogenous leukemia. *J Immunol.* 2004;173:5036-5045.

51. Gu W, Weihrauch D, Tanaka K, Tessmer JP, Pagel PS, Kersten JR, Chilian WM, Warltier DC. Reactive oxygen species are critical mediators of coronary collateral development in a canine model. *Am J Physiol Heart Circ Physiol.* 2003;285:H1582-1589.

52. Conway EM, Collen D, Carmeliet P. Molecular mechanisms of blood vessel growth. *Cardiovasc Res.* 2001;49:507-521.

53. Berton G, Mocsai A, Lowell CA. Src and Syk kinases: key regulators of phagocytic cell activation. *Trends Immunol.* 2005;26:208-214.

54. Zhu Q-s, Xia L, Mills GB, Lowell CA, Touw IP, Corey SJ. G-CSF induced reactive oxygen species involves Lyn-PI3-kinase-Akt and contributes to myeloid cell growth. *Blood.* 2006;107:1847-1856.

55. Steinfeld JL. Principles of Hematology. *Cancer Res.* 1967;27:208-a-.

56. Witko-Sarsat V, Rieu P, Descamps-Latscha B, Lesavre P, Halbwachs-Mecarelli L. Neutrophils: Molecules, Functions and Pathophysiological Aspects. *Lab Invest.* 2000;80:617-653.

57. Roos D, Bruggena Rv, Meischl C. Oxidative killing of microbes by neutrophils. *Microbes and Infection.* 2003;5:1307-1315.

58. Thannickal VJ, Fanburg BL. Reactive oxygen species in cell signaling. *Am J Physiol Lung Cell Mol Physiol.* 2000;279:L1005-1028.

59. Bedard K, Krause K-H. The NOX Family of ROS-Generating NADPH Oxidases: Physiology and Pathophysiology. *Physiol. Rev.* 2007;87:245-313.

60. Quinn MT, Gauss KA. Structure and regulation of the neutrophil respiratory burst oxidase: comparison with nonphagocyte oxidases. *J Leukoc Biol.* 2004;76:760-781.

61. Babior BM. NADPH oxidase. *Current Opinion in Immunology.* 2004;16:42-47.

62. Lambeth JD, Cheng G, Arnold RS, Edens WA. Novel homologs of gp91phox. *Trends Biochem Sci.* 2000;25:459-461.

63. Krijnen PA, Meischl C, Hack CE, Meijer CJ, Visser CA, Roos D, Niessen HW. Increased Nox2 expression in human cardiomyocytes after acute myocardial infarction. *J Clin Pathol.* 2003;56:194-199.

64. Ohki Y HB, Sato Y, Akiyama H, Zhu Z, Hicklin DJ, Shimada K, Ogawa H, Daida H, Hattori K, Ohsaka A. . Granulocyte colony-stimulating factor promotes neovascularization by releasing vascular endothelial growth factor from neutrophils. *FASEB J.* 2005;19:2005-2007.

65. Orlic D, Kajstura J, Chimenti S, Jakoniuk I, Anderson SM, Li B, Pickel J, McKay R, Nadal-Ginard B, Bodine DM, Leri A, Anversa P. Bone marrow cells regenerate infarcted myocardium. *Nature.* 2001;410:701-705.

66. Orlic D KJ, Chimenti S, Limana F, Jakoniuk I, Quaini F, Nadal-Ginard B, Bodine DM, Leri A, Anversa P. . Mobilized bone marrow cells repair the infarcted heart, improving function and survival. *Proc Natl Acad Sci U S A.* 2001;98:10344-10349.

67. Murry CE, Soonpaa MH, Reinecke H, Nakajima H, Nakajima HO, Rubart M, Pasumarthi KBS, Ismail Virag J, Bartelmez SH, Poppa V, Bradford G, Dowell JD, Williams DA, Field LJ. Haematopoietic stem cells do not transdifferentiate into cardiac myocytes in myocardial infarcts. *Nature.* 2004;428:664-668.

68. Balsam LB, Wagers AJ, Christensen JL, Kofidis T, Weissman IL, Robbins RC. Haematopoietic stem cells adopt mature haematopoietic fates in ischaemic myocardium. *Nature.* 2004;428:668-673.

69. Iwanaga K, Takano H, Ohtsuka M, Hasegawa H, Zou Y, Qin Y, Odaka K, Hiroshima K, Tadokoro H, Komuro I. Effects of G-CSF on cardiac remodeling after acute myocardial infarction in swine. *Biochem Biophys Res Commun.* 2004;325:1353-1359.

70. Ueda K TH, Hasegawa H, Niitsuma Y, Qin Y, Ohtsuka M, Komuro I. . Granulocyte colony stimulating factor directly inhibits myocardial ischemia-reperfusion injury through Akt-endothelial NO synthase pathway. *Arterioscler Thromb Vasc Biol.* . 2006;26:e108-113.

71. Haghighat A WD, Whalin MK, Cowan DP, Taylor WR. . Granulocyte colony-stimulating factor and granulocyte macrophage colony-stimulating factor exacerbate atherosclerosis in apolipoprotein E-deficient mice. *Circulation.* 2007;115:2049-2054.

72. Herrmann J, Lerman LO, Rodriguez-Porcel M, Holmes DR, Jr., Richardson DM, Ritman EL, Lerman A. Coronary vasa vasorum neovascularization precedes epicardial endothelial dysfunction in experimental hypercholesterolemia. *Cardiovasc Res.* 2001;51:762-766.

73. Kwon HM, Sangiorgi G, Ritman EL, McKenna C, Holmes DR, Jr., Schwartz RS, Lerman A. Enhanced coronary vasa vasorum neovascularization in experimental hypercholesterolemia. *J Clin Invest.* 1998;101:1551-1556.

74. Risau W. Mechanisms of angiogenesis. *Nature.* 1997;386:671-674.

75. Fong GH, Rossant J, Gertsenstein M, Breitman ML. Role of the Flt-1 receptor tyrosine kinase in regulating the assembly of vascular endothelium. *Nature.* 1995;376:66-70.

76. Carmeliet P, Conway EM. Growing better blood vessels. *Nat Biotechnol.* 2001;19:1019-1020.

77. Jones CJ, Kuo L, Davis MJ, DeFily DV, Chilian WM. Role of nitric oxide in the coronary microvascular responses to adenosine and increased metabolic demand. *Circulation.* 1995;91:1807-1813.

78. Liu Y, Cox SR, Morita T, Kourembanas S. Hypoxia regulates vascular endothelial growth factor gene expression in endothelial cells. Identification of a 5' enhancer. *Circ Res.* 1995;77:638-643.

79. Ben-Yosef Y, Lahat N, Shapiro S, Bitterman H, Miller A. Regulation of endothelial matrix metalloproteinase-2 by hypoxia/reoxygenation. *Circ Res.* 2002;90:784-791.

80. ten Dijke P, Arthur HM. Extracellular control of TGFbeta signalling in vascular development and disease. *Nat Rev Mol Cell Biol.* 2007;8:857-869.

81. Bloor CM, Liebow AA. Coronary Collateral Circulation. *Am J Cardiol.* 1965;16:238-252.

82. Bloor CM. Functional significance of the coronary collateral circulation. A review. *Am J Pathol.* 1974;76:561-588.

83. Koerselman J vdGY, de Jaegere PP, Grobbee DE. Coronary collaterals: an important and underexposed aspect of coronary artery disease. *Circulation.* . 2003 107:2507-2511.

84. Sasayama S, Fujita M. Recent insights into coronary collateral circulation. *Circulation.* 1992;85:1197-1204.

85. Yun J, Pung YF, Belmadani S, Carrao ACR, Rocic P, Chilian WM. Redox-Dependent Mechanisms in Coronary Collateral Growth: the "Redox Window" Hypothesis. *Antioxidants and Redox Signaling.28 Feb* 2009;ARS-2009-2476.

86. Pipp F, Boehm S, Cai WJ, Adili F, Ziegler B, Karanovic G, Ritter R, Balzer J, Scheler C, Schaper W, Schmitz-Rixen T. Elevated fluid shear stress enhances postocclusive collateral artery growth and gene expression in the pig hind limb. *Arterioscler Thromb Vasc Biol.* 2004;24:1664-1668.

87. Chilian WM MH, Williams SE, Layne SM, Smith EE, Scheel KW. . Microvascular occlusions promote coronary collateral growth. *Am J Physiol.* . 1990;1990:H1103-1111.

88. Birnbaum Y, Hale SL, Kloner RA. Ischemic preconditioning at a distance: reduction of myocardial infarct size by partial reduction of blood supply combined with rapid stimulation of the gastrocnemius muscle in the rabbit. *Circulation.* 1997;96:1641-1646.

89. Gho BC, Schoemaker RG, van den Doel MA, Duncker DJ, Verdouw PD. Myocardial protection by brief ischemia in noncardiac tissue. *Circulation.* 1996;94:2193-2200.

90. Verdouw PD, Gho BC, Koning MM, Schoemaker RG, Duncker DJ. Cardioprotection by ischemic and nonischemic myocardial stress and ischemia in remote organs. Implications for the concept of ischemic preconditioning. *Ann N Y Acad Sci.* 1996;793:27-42.

91. Helisch A, Wagner S, Khan N, Drinane M, Wolfram S, Heil M, Ziegelhoeffer T, Brandt U, Pearlman JD, Swartz HM, Schaper W. Impact of mouse strain differences in innate hindlimb collateral vasculature. *Arterioscler Thromb Vasc Biol.* 2006;26:520-526.

92. Cai Z, Zhong H, Bosch-Marce M, Fox-Talbot K, Wang L, Wei C, Trush MA, Semenza GL. Complete loss of ischaemic preconditioning-induced cardioprotection in mice with partial deficiency of HIF-1{alpha}. *Cardiovasc Res.* 2008;77:463-470.

93. Matsunaga T, Warltier DC, Weihrauch DW, Moniz M, Tessmer J, Chilian WM. Ischemia-induced coronary collateral growth is dependent on vascular endothelial growth factor and nitric oxide. *Circulation.* 2000;102:3098-3103.

94. Kappel A, Ronicke V, Damert A, Flamme I, Risau W, Breier G. Identification of Vascular Endothelial Growth Factor (VEGF) Receptor-2 (Flk-1) Promoter/Enhancer Sequences Sufficient for Angioblast and Endothelial Cell-Specific Transcription in Transgenic Mice. *Blood.* 1999;93:4284-4292.

95. Matsunaga T, Warltier DC, Tessmer J, Weihrauch D, Simons M, Chilian WM. Expression of VEGF and angiopoietins-1 and -2 during ischemia-induced coronary angiogenesis. *Am J Physiol Heart Circ Physiol.* 2003;285:H352-358.

96. Toyota E, Warltier DC, Brock T, Ritman E, Kolz C, O'Malley P, Rocic P, Focardi M, Chilian WM. Vascular endothelial growth factor is required for coronary collateral growth in the rat. *Circulation.* 2005;112:2108-2113.

97. Murphy E, Steenbergen C. Mechanisms Underlying Acute Protection From Cardiac Ischemia-Reperfusion Injury. *Physiol. Rev.* 2008;88:581-609.

98. Morrell CN. Reactive Oxygen Species: Finding the Right Balance. *Circ Res.* 2008;103:571-572.

99. Yamaoka-Tojo M, Ushio-Fukai M, Hilenski L, Dikalov SI, Chen YE, Tojo T, Fukai T, Fujimoto M, Patrushev NA, Wang N, Kontos CD, Bloom GS, Alexander RW. IQGAP1, a novel vascular endothelial growth factor receptor binding protein, is involved in reactive oxygen species--dependent endothelial migration and proliferation. *Circ Res.* 2004;95:276-283.

100. Tojo T, Ushio-Fukai M, Yamaoka-Tojo M, Ikeda S, Patrushev N, Alexander RW. Role of gp91phox (Nox2)-Containing NAD(P)H Oxidase in Angiogenesis in Response to Hindlimb Ischemia. *Circulation.* 2005;111:2347-2355.

101. Tuttle JL, Sanders BM, Burkhart HM, Fath SW, Kerr KA, Watson WC, Herring BP, Dalsing MC, Unthank JL. Impaired collateral artery development in spontaneously hypertensive rats. *Microcirculation.* 2002;9:343-351.

102. Tuttle JL, Hahn TL, Sanders BM, Witzmann FA, Miller SJ, Dalsing MC, Unthank JL. Impaired collateral development in mature rats. *Am J Physiol Heart Circ Physiol.* 2002;283:H146-155.

103. Becker LB, vanden Hoek TL, Shao Z-H, Li C-Q, Schumacker PT. Generation of superoxide in cardiomyocytes during ischemia before reperfusion. *Am J Physiol Heart Circ Physiol.* 1999;277:H2240-2246.

104. Eaton P, Hearse DJ, Shattock MJ. Lipid hydroperoxide modification of proteins during myocardial ischaemia. *Cardiovasc Res.* 2001;51:294-303.

105. Li Y, Wu J, Shou Z, He Q, Zhang P, Han FEI, Li HEN, Chen J. Pretreatment with granulocyte colony-stimulating factor attenuated renal ischaemia and reperfusion injury via activation of PI3/Akt signal pathway. *Nephrology.* 2008;0:???-???

106. Erdogan H, Fadillioglu E, Yagmurca M, Ucar M, Irmak MK. Protein oxidation and lipid peroxidation after renal ischemia-reperfusion injury: protective effects of erdosteine and N-acetylcysteine. *Urol Res.* 2006;34:41-46.

107. Reimer KA, Murry CE, Yamasawa I, Hill ML, Jennings RB. Four brief periods of myocardial ischemia cause no cumulative ATP loss or necrosis. *Am J Physiol.* 1986;251:H1306-1315.

108. Maulik N, Yoshida T, Zu YL, Sato M, Banerjee A, Das DK. Ischemic preconditioning triggers tyrosine kinase signaling: a potential role for MAPKAP kinase 2. *Am J Physiol.* 1998;275:H1857-1864.

109. Maulik N, Yoshida T, Engelman RM, Deaton D, Flack JE, 3rd, Rousou JA, Das DK. Ischemic preconditioning attenuates apoptotic cell death associated with ischemia/reperfusion. *Mol Cell Biochem.* 1998;186:139-145.

110. Chen W, Gabel S, Steenbergen C, Murphy E. A redox-based mechanism for cardioprotection induced by ischemic preconditioning in perfused rat heart. *Circ Res.* 1995;77:424-429.

111. Pain T, Yang XM, Critz SD, Yue Y, Nakano A, Liu GS, Heusch G, Cohen MV, Downey JM. Opening of mitochondrial K(ATP) channels triggers the preconditioned state by generating free radicals. *Circ Res.* 2000;87:460-466.

112. Hausenloy DJ, Tsang A, Mocanu MM, Yellon DM. Ischemic preconditioning protects by activating prosurvival kinases at reperfusion. *Am J Physiol Heart Circ Physiol.* 2005;288:H971-976.

113. Hausenloy DJ, Yellon DM, Mani-Babu S, Duchen MR. Preconditioning protects by inhibiting the mitochondrial permeability transition. *Am J Physiol Heart Circ Physiol.* 2004;287:H841-849.

114. Penna C, Rastaldo R, Mancardi D, Raimondo S, Cappello S, Gattullo D, Losano G, Pagliaro P. Post-conditioning induced cardioprotection requires signaling through a redox-sensitive mechanism, mitochondrial ATP-sensitive K+ channel and protein kinase C activation. *Basic Res Cardiol.* 2006;101:180-189.

115. Liu F, Patient R. Genome-Wide Analysis of the Zebrafish ETS Family Identifies Three Genes Required for Hemangioblast Differentiation or Angiogenesis. *Circ Res.* 2008:CIRCRESAHA.108.179713.

116. Petit I, Szyper-Kravitz M, Nagler A, Lahav M, Peled A, Habler L, Ponomaryov T, Taichman RS, Arenzana-Seisdedos F, Fujii N, Sandbank J, Zipori D, Lapidot T. G-CSF induces stem cell mobilization by decreasing bone marrow SDF-1 and up-regulating CXCR4. *Nat Immunol.* 2002;3:687-694.

117. Greene EL, Velarde V, Jaffa AA. Role of reactive oxygen species in bradykinin-induced mitogen-activated protein kinase and c-fos induction in vascular cells. *Hypertension.* 2000;35:942-947.

118. Velarde V, de la Cerda PM, Duarte C, Arancibia F, Abbott E, Gonzalez A, Moreno F, Jaffa AA. Role of reactive oxygen species in bradykinin-induced proliferation of vascular smooth muscle cells. *Biol Res.* 2004;37:419-430.

119. Ruiz-Gines JA, Lopez-Ongil S, Gonzalez-Rubio M, Gonzalez-Santiago L, Rodriguez-Puyol M, Rodriguez-Puyol D. Reactive oxygen species induce proliferation of bovine aortic endothelial cells. *J Cardiovasc Pharmacol.* 2000;35:109-113.

120. Gu W, Weihrauch D, Tanaka K, Tessmer JP, Pagel PS, Kersten JR, Chilian WM, Warltier DC. Reactive oxygen species are critical mediators of coronary collateral development in a canine model. *Am J Physiol Heart Circ Physiol.* 2003;285:H1582-1589.

121. Rocic P KC, Reed RE, Potter B, Chilian WM. Optimal reactive oxygen species concentration and p38 MAP kinase are required for coronary collateral growth. *Am J Physiol Heart Circ Physiol. .* 2007;Epub ahead of print.

122. Spaan JA tWR, van Teeffelen JW, Streekstra G, Siebes M, Kolyva C, Vink H, Fokkema DS, VanBavel E. Visualisation of intramural coronary vasculature by an imaging cryomicrotome suggests compartmentalisation of myocardial perfusion areas. *Med Biol Eng Comput. .* 2005;43:431-435.

123. De Greef KE, Ysebaert DK, Ghielli M, Vercauteren S, Nouwen EJ, Eyskens EJ, De Broe ME. Neutrophils and acute ischemia-reperfusion injury. *J Nephrol.* 1998;11:110-122.

124. Weihrauch D, Tessmer J, Warltier DC, Chilian WM. Repetitive coronary artery occlusions induce release of growth factors into the myocardial interstitium. *Am J Physiol.* 1998;275:H969-976.

125. Rocic P, Kolz C, Reed R, Potter B, Chilian WM. Optimal reactive oxygen species concentration and p38 MAP kinase are required for coronary collateral growth. *Am J Physiol Heart Circ Physiol.* 2007;292:H2729-2736.

126. Korpisalo P, Karvinen H, Rissanen TT, Kilpijoki J, Marjomaki V, Baluk P, McDonald DM, Cao Y, Eriksson U, Alitalo K, Yla-Herttuala S. Vascular Endothelial Growth Factor-A and Platelet-Derived Growth Factor-B Combination Gene Therapy Prolongs Angiogenic Effects via Recruitment of Interstitial Mononuclear Cells and Paracrine Effects Rather Than Improved Pericyte Coverage of Angiogenic Vessels. *Circ Res.* 2008:CIRCRESAHA.108.182287.

127. Koneru S, Penumathsa SV, Thirunavukkarasu M, Samuel SM, Zhan L, Han Z, Maulik G, Das DK, Maulik N. Redox regulation of ischemic preconditioning is mediated by the differential activation of caveolins and their association with eNOS and GLUT-4. *Am J Physiol Heart Circ Physiol.* 2007;292:H2060-2072.

128. Powell TM PJ, Hill JM, Thompson M, Benjamin M, Rodrigo M, McCoy JP, Read EJ, Khuu HM, Leitman SF, Finkel T, Cannon RO 3rd. . Granulocyte colony-stimulating factor mobilizes functional endothelial progenitor cells in patients with coronary artery disease. *Arterioscler Thromb Vasc Biol.* 2005;25:296-301.

129. Ximenes VF, Kanegae MP, Rissato SR, Galhiane MS. The oxidation of apocynin catalyzed by myeloperoxidase: proposal for NADPH oxidase inhibition. *Arch Biochem Biophys.* 2007;457:134-141.

130. Touyz RM. Apocynin, NADPH Oxidase, and Vascular Cells: A Complex Matter. *Hypertension.* 2008;51:172-174.

131. Stolk J, Hiltermann TJ, Dijkman JH, Verhoeven AJ. Characteristics of the inhibition of NADPH oxidase activation in neutrophils by apocynin, a methoxy-substituted catechol. *Am. J. Respir. Cell Mol. Biol.* 1994;11:95-102.

132. Heymes C, Bendall JK, Ratajczak P, Cave AC, Samuel JL, Hasenfuss G, Shah AM. Increased myocardial NADPH oxidase activity in human heart failure. *J Am Coll Cardiol.* 2003;41:2164-2171.

133. Elisabetta Borchi MPLPMBNNPNCN. Role of NADPH oxidase in H9c2 cardiac muscle cells exposed to simulated ischemia-reperfusion. *Journal of Cellular and Molecular Medicine.* 2008;9999.

134. Boneberg E-M, Hareng L, Gantner F, Wendel A, Hartung T. Human monocytes express functional receptors for granulocyte colony- stimulating factor that mediate suppression of monokines and interferon-gamma. *Blood.* 2000;95:270-276.

135. Nicholls SJ, Hazen SL. Myeloperoxidase and Cardiovascular Disease. *Arterioscler Thromb Vasc Biol.* 2005;25:1102-1111.

136. Ripa RS, Kastrup J. G-CSF therapy with mobilization of bone marrow stem cells for myocardial recovery after acute myocardial infarction--a relevant treatment? *Exp Hematol.* 2008;36:681-686.

137. Zohlnhofer D, Dibra A, Koppara T, de Waha A, Ripa RS, Kastrup J, Valgimigli M, Schomig A, Kastrati A. Stem cell mobilization by granulocyte colony-stimulating factor for myocardial recovery after acute myocardial infarction: a meta-analysis. *J Am Coll Cardiol.* 2008;51:1429-1437.

138. Kurdi M, Booz GW. G-CSF-based stem cell therapy for the heart-unresolved issues part A: paracrine actions, mobilization, and delivery. *Congest Heart Fail.* 2007;13:221-227.

9. Appendix

9.1 Data for hematological profile of groups

Before Surgery:						
Animal	**WBC**	**Neutrophils**	**Lymphocytes**	**Monocytes**	**Eosinophils**	**Basophils**
CC50	7.86	1.88	5.58	0.36	0.03	0.01
CC51	8.86	2.43	6.14	0.19	0.08	0.02
CC52	11.34	2.84	7.89	0.57	0.04	0.01
CC53	7.26	1.69	5.23	0.28	0.05	0.01
CC56	13.20	2.18	10.24	0.47	0.24	0.06
CC57	9.66	1.35	7.67	0.56	0.06	0.02
Average	10.15	2.13	7.40	0.46	0.12	0.04
StanDev	2.23	0.59	1.78	0.19	0.10	0.04

Table 2 – Results from haematological profile obtained before surgery (units K/μL). WBC=White Blood cell count

Vehicle +RI						
Animal	**WBC**	**Neutrophils**	**Lymphocytes**	**Monocytes**	**Eosinophils**	**Basophils**
CC33	21.12	12.27	7.58	0.91	0.24	0.11
CC40	19.08	12.72	5.13	0.58	0.58	0.07
CC50	16.16	9.66	5.58	0.58	0.22	0.12
CC64	17.64	10.40	5.59	0.75	0.74	0.15
CC83	21.20	15.81	4.15	1.09	0.07	0.08
CC84	16.16	10.56	4.45	1.06	0.07	0.01
Average	19.19	11.65	5.94	0.78	0.24	0.06
StanDev	3.44	1.85	1.81	0.22	0.22	0.04

Table 3 – Results from haematological profile obtained for animals treated with Vehicle + Repetitive Ischemia (units K/μL). WBC=White Blood cell count

G-CSF + RI						
Animal	**WBC**	**Neutrophils**	**Lymphocytes**	**Monocytes**	**Eosinophils**	**Basophils**
CC37	28.20	20.87	5.14	0.60	1.46	0.13
CC46	29.08	19.60	7.49	0.95	0.88	0.17
CC74	18.34	13.48	3.75	0.51	0.54	0.07
CC75	28.62	16.70	10.17	0.92	0.53	0.29
CC78	23.16	16.24	5.73	0.78	0.30	0.12
CC79	27.86	19.20	7.18	0.62	0.64	0.22
CC82	21.34	12.63	7.81	0.54	0.20	0.15
Average	26.66	18.05	6.92	0.89	0.65	0.15
StanDev	5.04	3.84	2.19	0.31	0.50	0.08

Table 4 – Results from haematological profile obtained for animals treated with G-CSF + Repetitive Ischemia (units K/μL). WBC=White Blood cell count

G-CSF						
Animal	**WBC**	**Neutrophils**	**Lymphocytes**	**Monocytes**	**Eosinophils**	**Basophils**
CC62	25.76	17.04	7.30	0.84	0.41	0.16
CC65	24.08	16.10	6.60	0.85	0.43	0.10
CC69	24.98	14.72	7.85	0.63	1.66	0.13
CC95	21.20	11.36	8.56	0.88	0.32	0.08
CC96	30.28	20.03	8.40	0.91	0.76	0.17
CC97	23.90	14.04	8.40	0.91	0.43	0.12
Average	25.08	15.12	8.33	0.84	0.66	0.12
StanDev	2.82	2.61	1.69	0.14	0.48	0.04

Table 5 – Results from haematological profile obtained for animals treated with G-CSF (units K/μL). WBC=White Blood cell count

G-CSF+RI+Apocynin						
Animal	**WBC**	**Neutrophils**	**Lymphocytes**	**Monocytes**	**Eosinophils**	**Basophils**
CC122	13.74	6.58	7.18	0.89	0.24	0.1
CC123	13.92	4.05	6.3	0.71	0.22	0.07
CC124	6.02	2.81	2.87	0.637	0.03	0.01
Average	11.227	4.480	5.450	0.746	0.163	0.060
StanDev	4.510	1.921	2.277	0.130	0.116	0.046

Table 6 – Results from haematological profile obtained for animals treated with G-CSF + Repetitive Ischemia + Apocynin (units K/μL). WBC=White Blood cell count

G-CSF +Apocynin						
Animal	**WBC**	**Neutrophils**	**Lymphocytes**	**Monocytes**	**Eosinophils**	**Basophils**
CC125	16.6	6.68	8.9	0.86	0.11	0.06
CC126	7.62	1.58	5.59	0.39	0.05	0.02
CC127	14.79	6.75	6.62	1.26	0.14	0.12
Average	13.003	5.003	7.037	0.837	0.100	0.067
StanDev	4.749	2.965	1.694	0.435	0.046	0.050

Table 7 – Results from haematological profile obtained for animals treated with G-CSF + Apocynin (units K/μL). WBC=White Blood cell count

9.2 Data for Coronary Collateral Blood Flow measurements

Vehicle + RI			
Sample	**Before treatment**	**After treatment**	**Delta**
CC33	0.3649	0.5122	0.1474
CC40	0.1586	0.2382	0.0796
CC50	0.9261	1.0831	0.1570
CC64	0.5015	0.7346	0.2330
CC83	0.4301	0.5808	0.1507
CC84	0.4803	0.5463	0.0660
		Average	0.1390
		StandDev	0.0604

Table 8 – Results from coronary collateral blood flow analysis for Vehicle + Repetitive Ischemia treated animals by injection of 15 μm microspheres in the left ventricle before and after treatments

G-CSF+RI			
Sample	**Before treatment**	**After treatment**	**Delta**
CC37	0.3595	1.0161	0.6566
CC46	0.4794	0.9316	0.4522
CC74	0.9574	1.2561	0.4743
CC75	0.4270	1.1189	0.6919
CC78	0.8164	1.1408	0.3243
CC79	0.3324	0.6390	0.3066
CC82	0.5983	1.0127	0.4144
		Average	0.4743
		StandDev	0.1531

Table 9 – Results from coronary collateral blood flow analysis for G-CSF + Repetitive Ischemia treated animals by injection of 15 μm microspheres in the left ventricle before and after treatments

G-CSF			
Sample	**Before treatment**	**After treatment**	**Delta**
CC62	0.6949	1.1761	0.4812
CC65	0.5096	1.3936	0.8840
CC69	0.6296	0.9635	0.3339
CC95	0.5395	0.2646	0.5664
CC96	0.3775	0.2382	0.5664
CC97	3.2543	0.6798	0.5664
		Average	0.5664
		StandDev	0.1801

Table 10 – Results from coronary collateral blood flow analysis for G-CSF treated animals by injection of 15 μm microspheres in the left ventricle before and after treatments

G-CSF+RI+Apocynin			
Sample	**Before treatment**	**After treatment**	**Delta**
CC122	0.241	0.390	0.131
CC123	1.266	1.376	0.110
CC124	0.935	1.067	0.132
		Average	0.124
		StandDev	0.0120

Table 11 – Results from coronary collateral blood flow analysis for G-CSF + Repetitive Ischemia + Apocynin treated animals by injection of 15 μm microspheres in the left ventricle before and after treatments

G-CSF +Apocynin			
Sample	**Before treatment**	**After treatment**	**Delta**
CC125	1.303	1.445	0.126
CC126	0.852	0.990	0.138
CC127	0.327	0.426	0.099
		Average	0.121
		StandDev	0.019732614

Table 12 – Results from coronary collateral blood flow analysis for G-CSF + Apocynin treated animals by injection of 15 μm microspheres in the left ventricle before and after treatments

9.3 Data for Fluorescence levels of Dihydroethidium (DHE) for ROS detection

Vehicle + RI	Fluorescence level
CC89	40.618767
CC87	36.863108
CC91	44.374427
Average	40.618767
StanDev	3.756

Table 13 – Results from fluorescence levels of DHE for Vehicle + Repetitive Ischemia treated animals measured in grey scale units

G-CSF + RI	Fluorescence level
CC92	81.413755
CC88	83.338518
CC94	78.246799
Average	80.999690
StanDev	2.571

Table 14 – Results from fluorescence levels of DHE for G-CSF + Repetitive Ischemia treated animals measured in grey scale units

G-CSF	Fluorescence level
CC110	106.197653
CC108	118.234382
CC106	99.270867
Average	107.900967
StanDev	9.596

Table 15 – Results from fluorescence levels of DHE for G-CSF treated animals measured in grey scale units

G-CSF + RI + Apocynin	Fluorescence level
CC122	30.71992667
CC123	30.04775333
CC124	31.16567667
Average	30.64445222
StanDev	0.562

Table 16 – Results from fluorescence levels of DHE for G-CSF + Repetitive Ischemia + Apocynin treated animals measured in grey scale units

G-CSF + Apocynin	Fluorescence level
CC125	21.23799333
CC126	37.38797667
CC127	36.26081889
Average	31.62892963
StanDev	9.016445475

Table 17 – Results from fluorescence levels of DHE for G-CSF + Apocynin treated animals measured in grey scale units

9.4 Data for tube formation assays

(-) Control Regular medium	No. Squares covered	% area covered (-) Control
Assay 1	4	0.171159606
Assay 2	6	0.256739409
Assay 3	8	0.342319213
Assay 4	4	0.171159606
	Average	0.235344459
	StanDev	0.081936423

Table 18 – Results from percentage of area covered with tubes by Human coronary artery endothelial cell (HCAEC) in Matrigel to a total area of 2337 squares using Regular Medium as negative control

(+) Control VEGF	No. Squares covered	% area covered (+) Control
Assay 1	116	4.963628584
Assay 2	112	4.792468977
Assay 3	113	4.835258879
Assay 4	171	7.317073171
	Average	5.477107403
	StanDev	1.228798034

Table 19 – Results from percentage of area covered with tubes by Human coronary artery endothelial cell (HCAEC) in Matrigel to a total area of 2337 squares using VEGF as positive control

G-CSF 2h	No. Squares covered	% area covered G-CSF 2h
Assay 1	195	8.344030809
Assay 2	129	5.519897304
Assay 3	95	4.06504065
Assay 4	107	4.578519469
	Average	5.626872058
	StanDev	1.908992384

Table 20 – Results from percentage of area covered with tubes by Human coronary artery endothelial cell (HCAEC) in Matrigel to a total area of 2337 squares using 2h G-CSF cardiomyocyte stimulation media

G-CSF 2h + Apocynin	No. Squares covered	% area covered G-CSF 2h + Apocynin
Assay 1	22	0.941377835
Assay 2	21	0.898587933
Assay 3	27	1.155327343
Assay.4	23	0.984167736
	Average	0.994865212
	StanDev	0.112535543

Table 21 – Results from percentage of area covered with tubes by Human coronary artery endothelial cell (HCAEC) in Matrigel to a total area of 2337 squares using 2h G-CSF cardiomyocyte stimulation media + Apocynin

G-CSF 24h	No. squares covered	% area covered G-CSF 24h
Assay 1	242	10.35515618
Assay 2	214	9.157038939
Assay 3	221	9.45656825
Assay.4	234	10.01283697
	Average	9.745400086
	StanDev	0.539418716

Table 22 – Results from percentage of area covered with tubes by Human coronary artery endothelial cell (HCAEC) in Matrigel to a total area of 2337 squares using 24h G-CSF cardiomyocyte stimulation media

G-CSF 24h + Apocynin	No. Squares covered	% area covered G-CSF 24h + Apocynin
Assay 1	17	0.727428327
Assay 2	24	1.026957638
Assay 3	23	0.984167736
Assay 4	21	0.898587933
	Average	0.909285409
	StanDev	0.132464524

Table 23 – Results from percentage of area covered with tubes by Human coronary artery endothelial cell (HCAEC) in Matrigel to a total area of 2337 squares using 24h G-CSF cardiomyocyte stimulation media + Apocynin

9.5 Statistical analysis

9.5.1 Hematology

T Test: Neutrophils	p value	
Vehicle vs G-CSF+RI	8.59596E-07	<0.01
Vehicle vs G-CSF NoRI	0.000153572	<0.01
G-CSF+RI vs G-CSF NoRI	0.294663724	>0.05
G-CSF+RI vs G-CSF+RI+Apocynin	0.005993006	<0.01
G-CSF NoRI vs G-CSF NoRI+Apocynin	0.003997508	<0.01

Table 24 – Results from T test performed for neutrophils levels between groups of study

T Test: Monocytes	p value	
Vehicle vs G-CSF+RI	0.933817265	>0.05
Vehicle vs G-CSF NoRI	0.457934693	>0.05
G-CSF+RI vs G-CSF NoRI	0.241239673	>0.05
G-CSF+RI vs G-CSF+RI+Apocynin	0.721392465	>0.05
G-CSF NoRI vs G-CSF NoRI+Apocynin	0.687381722	>0.05

Table 25 – Results from T test performed for monocytes levels between groups of study

T Test: Eosinophils	p value	
Vehicle vs G-CSF+RI	0.171288592	>0.05
Vehicle vs G-CSF NoRI	0.171656583	>0.05
G-CSF+RI vs G-CSF NoRI	0.940223752	>0.05
G-CSF+RI vs G-CSF+RI+Apocynin	0.024912169	<0.01
G-CSF NoRI vs G-CSF NoRI+Apocynin	0.071000838	<0.01

Table 26 – Results from T test performed for eosinophils levels between groups of study

T Test: Basophils	p value	
Vehicle vs G-CSF+RI	0.160551717	>0.05
Vehicle vs G-CSF NoRI	0.162448064	>0.05
G-CSF+RI vs G-CSF NoRI	0.576816668	>0.05
G-CSF+RI vs G-CSF+RI+Apocynin	0.182349882	>0.05
G-CSF NoRI vs G-CSF NoRI+Apocynin	0.13450004	>0.05

Table 27 – Results from T test performed for basophils levels between groups of study

9.5.2 Coronary Collateral Blood Flow assay

T Test	p value	
Vehicle vs G-CSF+RI	0.000342378	<0,05
Vehicle vs G-CSF NoRI	0.000257774	<0,05
G-CSF+RI vs G-CSF NoRI	0.336021653	>0,05
Vehicle vs Apocynin	0.041513766	<0,05

Table 28 – Results from T test performed between different groups of coronary collateral blood flow measurements

9.5.3 Dihydroethidine fluorescence assay

T test	p value	
Vehicle vs G-CSF+RI	0.000104619	<0,01
Vehicle vs G-CSF NoRI	0.000348439	<0,01
G-CSF+RI vs G-CSF NoRI	0.009375878	<0,01
G-CSF+RI vs Apocynin	4.94482E-06	<0,01
G-CSF NoRI vs Apocynin	0.000554876	<0,01

Table 29 – Results from T test performed between different groups of Dihydroethidine (DHE) fluorescence analysis

9.5.4 Human Coronary Artery Endothelial Cell tube formation assay

T test	p value	
VEGF vs G-CSF24h	0.00031468	<0,01
VEGF vs G-CSF2h	0.899349065	>0,05
G-CSF 2h vs 24h	0.005995771	<0,01
G-CSF 24h vs Apo group	6.40716E-08	<0,01
G-CSF 2h vs apo group	0.002867871	<0,01

Table 30 – Results from T test performed between different groups of Human Coronary Endothelial Cell (HCAEC) tube formation assay

Curriculum Vitae

For reasons of data protection,
the curriculum vitae is not included in the online version